

ENHANCEMENT OF PERFORMANCE CHARACTERISTICS OF EPOXY
ADHESIVES THROUGH PARTICLE REINFORCEMENT

A THESIS SUBMITTED TO
THE GRADUATE SCHOOL OF NATURAL AND APPLIED SCIENCES
OF
MIDDLE EAST TECHNICAL UNIVERSITY

BY

HASAN YETGİN

IN PARTIAL FULFILLMENT OF THE REQUIREMENTS
FOR
THE DEGREE OF MASTER OF SCIENCE
IN
AEROSPACE ENGINEERING

DECEMBER 2019

Approval of the thesis:

**ENHANCEMENT OF PERFORMANCE CHARACTERISTICS OF EPOXY
ADHESIVES THROUGH PARTICLE REINFORCEMENT**

submitted by **HASAN YETGİN** in partial fulfillment of the requirements for the degree of **Master of Science in Aerospace Engineering Department, Middle East Technical University** by,

Prof. Dr. Halil Kalıpçılar
Dean, Graduate School of **Natural and Applied Sciences**

Prof. Dr. İsmail H. Tuncer
Head of Department, **Aerospace Engineering**

Assoc. Prof. Dr. Tuncay Yalçınkaya
Supervisor, **Aerospace Engineering, METU**

Assoc. Prof. Dr. Oral Cenk Aktaş
Co-Supervisor, **Christian-Albert University**

Examining Committee Members:

Prof. Dr. Altan Kayran
Department of Aerospace Engineering, METU

Assoc. Prof. Dr. Tuncay Yalçınkaya
Aerospace Engineering, METU

Assoc. Prof. Dr. Ercan Gürses
Department of Aerospace Engineering, METU

Assoc. Prof. Dr. Demirkan Çöker
Department of Aerospace Engineering, METU

Assoc. Prof. Dr. Barış Sabuncuoğlu
Department of Mechanical Engineering, Hacettepe University

Date: 13.12.2019

I hereby declare that all information in this document has been obtained and presented in accordance with academic rules and ethical conduct. I also declare that, as required by these rules and conduct, I have fully cited and referenced all material and results that are not original to this work.

Name, Surname: Hasan Yetgin

Signature:

ABSTRACT

ENHANCEMENT OF PERFORMANCE CHARACTERISTICS OF EPOXY ADHESIVES THROUGH PARTICLE REINFORCEMENT

Yetgin, Hasan

Master of Science, Aerospace Engineering

Supervisor : Assoc. Prof. Dr. Tuncay Yalçınkaya

Co-Supervisor: Assoc. Prof. Dr. Oral Cenk Aktaş

December 2019, 66 pages

Epoxy adhesives are common bonding agents used to join dissimilar materials. They are widely preferred in aerospace industry. But, their lack of performance at extremities of service temperatures limits their use in practical applications. The aim of this study is to improve the epoxy adhesives' thermal properties through addition of filler particles, i.e. boron nitride, aluminum oxide, titanium oxide and Au doped titanium oxide. The last one has been developed specifically for this study to enhance the drawbacks of titanium particles in thermal conductivity. In order to have regular samples, a sample preparation method has been suggested. Then, the samples were tested by Dynamic Mechanical Analysis (DMA), Differential Scanning Calorimetry (DSC), Scanning Electron Microscopy (SEM), Thermal Conductivity Measurement, Fourier Transform Infrared Spectroscopy (FTIR) and Single Lap Shear Test. The results showed that adding filler materials had favorable influence on thermal and mechanical performance. For the key parameters of thermal and mechanical performance of adhesives, boron nitride particles had greatest influence on the thermal conductivity. Moreover, Au doped and regular titanium dioxide particles had

brilliant results in glass transition temperature. Adhesion strength was enhanced mostly by aluminum dioxide particles. The result of scanning methods validated the suggested sample preparation method. Finally, while Au doped titanium oxide particles enhanced the glass transition temperature, the expected improvement on thermal conductivity value has not been reached.

Keywords: Epoxy Reinforcement, Aerospace Industry, Particle Addition

ÖZ

EPOKSİ BAZLI YAPIŞTIRICILARIN PARÇACIK KATKISI İLE PERFORMANSININ GELİŞTİRİLMESİ

Yetgin, Hasan

Yüksek Lisans, Havacılık ve Uzay Mühendisliği

Tez Yöneticisi: Doç. Dr. Tuncay Yalçınkaya

Ortak Tez Yöneticisi: Doç. Dr. Oral Cenk Aktaş

Aralık 2019, 66 sayfa

Epoksi yapıştırıcılar benzer olmayan malzemelerin birbirine birleştirilmeleri için genel olarak kullanılan bir bağlantı elemanıdır. Ancak servis sıcaklıklarının sınırlarında yaşadıkları performans kayıpları kullanımlarını sınırlandırmaktadır. Bu çalışmanın amacı epoksi yapıştırıcıların termal özelliklerinin bor nitrür, alüminyum oksit, titanyum oksit ve altın kaplanmış titanyum oksit parçacıkları eklenerek geliştirilmesidir. Titanyum oksit parçacıklarının termal iletkenlik üzerindeki negatif etkilerinin giderilmesi için altın kaplı titanyum oksit parçacıkları özellikle geliştirilmiştir. Nizami numuneler elde edilebilmesi için bir numune hazırlama metodu da önerilmiştir. Sonrasında, numuneler DMA, DSC, Termal İletkenlik Ölçümü, SEM, FTIR ve Kesme deneyi ile test edilmiştir. Sonuçlar parçacık eklemenin termal ve mekanik özellikler üzerinde olumlu etkilere sahip olduğunu göstermiştir. Termal ve mekanik performansın anahtar parametreleri için; bor nitrür termal iletkenlik üzerine, altın kaplanmış titanyum oksit camsı geçiş sıcaklığı açısından ve alüminyum oksit yapışma mukavemeti açısından en çok geliştirmeyi göstermiştir. Görüntüleme yöntemleri ile de önerilen numune hazırlama metodu

doğrulanmıştır. Son olarak, altın kaplanmış titanyum oksit parçacıkları camsı geçiş sıcaklığını geliştirse de beklenenin termal iletkenlik değerine erişememiştir.

Anahtar Kelimeler: Epoksi Yapıştırıcı Güçlendirme, Havacılık Sanayi, Parçacık Ekleme

To whom lost in this way and lost his way

ACKNOWLEDGMENTS

First of all, I wish to express my genuine appreciation to my supervisor Assist. Prof. Dr. Tuncay Yalçınkaya for his guidance, advice, patience and faith throughout this work. His positive attitude and tolerance made me stand firm.

Also, I am grateful to my co-advisor Assoc. Prof. Dr. Oral Cenk Aktaş. His mentorship and logistic support made this work possible. Mr. Salih Veziroğlu has my gratitude for his help on laboratory work and precious comments on study.

I am thankful to laboratory staff from ROKETSAN for their support and allowance for tests. Also, I want to thank Tuncay Tunç for his supportive behavior to me and my work.

Grateful thanks go to my former fiancée and wife Fatoş Alev Yetgin for her support and faith during this work.

My friends and colleagues Tevfik Ozan Fenercioğlu, Hasan Baran Özmen, Denizhan Yerel, Ahmet Can Afatsun and Özkan Kahveci deserve grate gratitude. They always stand by with me. Also, tired and valuable thanks go to my bachelor's and master's fellow Burak Ogün Yavuz.

Lastly, I would like to thank to my father Mehmet, my mother Nurcan and my brothers Ali and Oğuzhan for their endless support and love. I could not achieve any of these without their support and belief in me.

TABLE OF CONTENTS

ABSTRACT	v
ÖZ	vii
ACKNOWLEDGEMENTS	x
TABLE OF CONTENTS	xi
LIST OF TABLES	xiii
LIST OF FIGURES	xiv
CHAPTERS	
1. INTRODUCTION	1
2. LITERATURE SURVEY	7
2.1. Aim of the Study	19
3. TEST METHODS.....	21
3.1. Dynamic Mechanical Analysis (DMA).....	21
3.2. Differential Scanning Calorimetry (DSC).....	23
3.3. Fourier Transform Infrared Spectrometer (FTIR).....	25
3.4. Thermal Conductivity (TC).....	26
3.5. Scanning Electron Microscope (SEM)	27
3.6. Single Lap Shear Test.....	28
4. MATERIALS AND PREPARATION METHODS	31
4.1. Materials	32
4.2. Sample Preparation Methods.....	32
4.2.1. Molds/Adherends Preparation	33
4.2.2. Particles Preparation	33

4.2.3. Composite Adhesive Preparation	34
5. RESULTS AND DISCUSSION	35
6. CONCLUSION	57
REFERENCES	63

LIST OF TABLES

TABLES

Table 2-1 Mechanical Properties of hBN filled Epoxy.....	9
Table 2-2 Test Specimens Composition	10
Table 2-3 Thermal Stability of Composite Adhesive	12
Table 2-4 Test Specimen Matrix.....	14
Table 2-5 Thermal Conductivity Values of TiO ₂ added Composite Adhesives	16
Table 2-6 TGA Values for Thermal Stability	17
Table 2-7 Test Results of Samples.....	17
Table 5-1 Glass Transition Values of All Samples.....	40
Table 5-2 Thermal Conductivity Values (W/m K) of Samples at Different Temperatures.....	41
Table 5-3 Maximum Shear Stress at Breakage of Samples	49

LIST OF FIGURES

FIGURES

Figure 1-1 Diagrammatic view of the de Havilland Comet and where structural adhesives used, (A) Canopy structure, (B) Longitudinal stringers of fuselage (C) Local doublers and reinforcements around windows (D,E,H,J,K) Spanwise stringers, ailerons and flap structures, vertical stiffener flanges in wings (F) Wall stiffeners in tail (G) Sealing in pressure dome (L) all stiffeners in pressure floor [1]	3
Figure 1-2 Schematic view of the Airbus A380 and adhesive bonding used areas[4]	3
Figure 2-1 Thermal Conductivity Values with increasing hBN ratio [16].	8
Figure 2-2 DSC Results with varying hBN ratio[16]	9
Figure 2-3 Tg Values from DSC Results with varying Al ₂ O ₃ Content[25]	11
Figure 2-4 Thermal Conductivity over Al ₂ O ₃ Content[26]	13
Figure 2-5 TiO ₂ +Au and Epoxy Interaction	19
Figure 3-1 ARES G2 Rheometer (https://www.tainstruments.com/ares-g2/)	22
Figure 3-2 DMA Sample	22
Figure 3-3 Example of DSC Plot.....	24
Figure 3-4 TA Instruments Q200 (yorku.ca/tbaumgar/photo/album/ta-instruments-dsc-q200)	24
Figure 3-5 DSC Sample.....	25
Figure 3-6 Bruker Tensor 27 FTIR Spectrometer(http://triadsci.com/en/products/ftir-ir-and-near-ir-spectroscopy/946/bruker-tensor-27-ftir-bruker-ftir-bruker-27/251160)	26
Figure 3-7 TA Instruments DTC-300 (https://www.tainstruments.com/dtc-300/)....	27
Figure 3-8 Thermal Conductivity Sample	27
Figure 3-9 Carl Zeiss Supra 55(https://www.cecni.res.in/SAIF/carl.html).....	28
Figure 3-10 Instron 5500R.....	29
Figure 3-11 Test Samples	29

Figure 4-1 Bubbled and Regular Samples	32
Figure 4-2 Molds of a) Thermal Inductivity b) FT-IR c) DSC d) DMA Tests	33
Figure 4-3 Example Schematic Presentation for the Sample Preparation	34
Figure 5-1 a) hBN particle b) Al ₂ O ₃ particle improvement on storage modulus	36
Figure 5-2 Loss Factor of Samples	37
Figure 5-3 a) Synergetic Mixture of hBN-Al ₂ O ₃ b) TiO ₂ and TiO ₂ +Au improvement	38
Figure 5-4 Storage modulus over temperature for all samples	39
Figure 5-5 Thermal Conductive Pathways in Composite Adhesive Structure	41
Figure 5-6 Reference FTIR Spectrum (http://what-when-how.com/wp-content/uploads/2011/06/tmp17058_thumb1.png)	42
Figure 5-7 FTIR Spectrum of Neat Epoxy	43
Figure 5-8 FTIR Spectra of Epoxy with hBN particles	44
Figure 5-9 FTIR Spectra of Epoxy with Al ₂ O ₃	44
Figure 5-10 FTIR Spectra of Synergetic Mixtures of hBN and Al ₂ O ₃	45
Figure 5-11 FTIR Spectra of TiO ₂ and Au-doped TiO ₂ Particles	46
Figure 5-12 SEM Screening of 20% hBN	47
Figure 5-13 SEM Images of 20% Al ₂ O ₃	47
Figure 5-14 SEM Screening of Synergetic Mixture	48
Figure 5-15 Single Lap Shear Test Setup	49
Figure 5-16 Example of Shear-Strain Curve	50
Figure 5-17 Fracture Surface of Neat Epoxy	51
Figure 5-18 Al ₂ O ₃ Particles' Effect on Shear Stress	52
Figure 5-19 Fracture Surfaces of Al ₂ O ₃ Samples	52
Figure 5-20 hBN Particles' Effect on Shear Stress	53
Figure 5-21 Fracture Surfaces of hBN Particles	53
Figure 5-22 The Synergetic Mixture's Effect on Shear Stress	54
Figure 5-23 Fracture Surfaces of Synergetic Mixtures	55
Figure 5-24 TiO ₂ Particles' Effect on Shear Stress	55
Figure 5-25 Fracture Surfaces of TiO ₂ Particles	56

CHAPTER 1

INTRODUCTION

The applications of the adhesives are constantly increasing in the aerospace industry. Even though, the history of the adhesive bonding dates back to the ancient times as structural reinforcement materials, the most important innovations were achieved in 19th century. In the beginning of 20th century, the Wright Brothers and their plane led onto a new industry called aviation. This new industry has led to the foundation of the aerospace industry and advanced material development programs.[1]

Moreover, they also strengthened their wooden plane by using some protein-based adhesives. They reduced the usage of mechanical fasteners that are used to join parts of the plane. Then, they made possible to construct the plane lighter, durable and stronger [1]. With the help of their applications, adhesives were introduced to the aviation industry. During two world wars, the aviation industry had an inevitable evolution from wooden airplanes to metallic ones. But the requirements remained the same, namely lighter, more durable and stronger planes. Moreover, more complicated and sophisticated adhesives were synthesized to satisfy the emerging requirements. After the World War II, a statement was made as structural adhesive bonding is a better option in aviation industry. The most important advantages over conventional connection methods such as bolting and/or riveting are summarized as follows [2]:

- Joining dissimilar materials
- Reduction in weight
- Better fatigue performances
- Design flexibility
- Well stress distribution over joint

- Smooth external finish
- Bonding thin substrates
- Cost and time effective
- Sealing in joint area
- Increased strength

Bonding is also used to support riveted structures against shear loading conditions. During the world wars, the development in aerospace companies were driven by defense and military contracts. However, by the end of the world wars era, the aerospace companies encountered financial problems due to lack of new contracts. Hence, a new path has emerged for the aerospace industry: commercial airplane programs. As a result of the commercial applications, new standards and certifications were constructed to ensure the safety.

Moreover, initial applications of the adhesive bonding were limited because of these performance validation and certification requirements of aerospace structures. This limitation was resolved by the development of new testing techniques such as dynamic mechanical analysis, differential scanning calorimetry, thermogravimetric analysis and thermal mechanical analysis. These techniques are mainly used to understand and characterize the behavior of adhesives under service. So, more systematic classification can be performed, and the usage of adhesives can be broadened in aerospace industry.

In 1949, the world's first commercial airliner with jet engine, the de Havilland Comet, was developed and manufactured. In the Figure 1-1, it can be seen at where adhesives were used as a joining agent [3].

In the modern era, awareness about adhesives was raised, and adhesives become stronger and found new areas of usage. In the Figure 1-2, a well-known airplane Airbus A380 and its parts with adhesives can be seen [4].

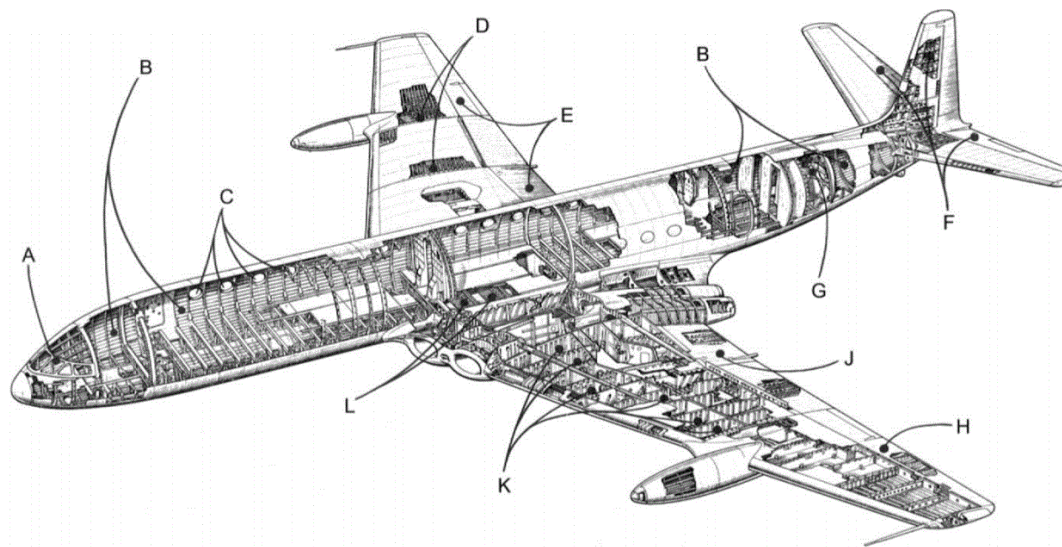


Figure 1-1 Diagrammatic view of the de Havilland Comet and where structural adhesives used, (A) Canopy structure, (B) Longitudinal stringers of fuselage (C) Local doublers and reinforcements around windows (D,E,H,J,K) Spanwise stringers, ailerons and flap structures, vertical stiffener flanges in wings (F) Wall stiffeners in tail (G) Sealing in pressure dome (L) all stiffeners in pressure floor [1]

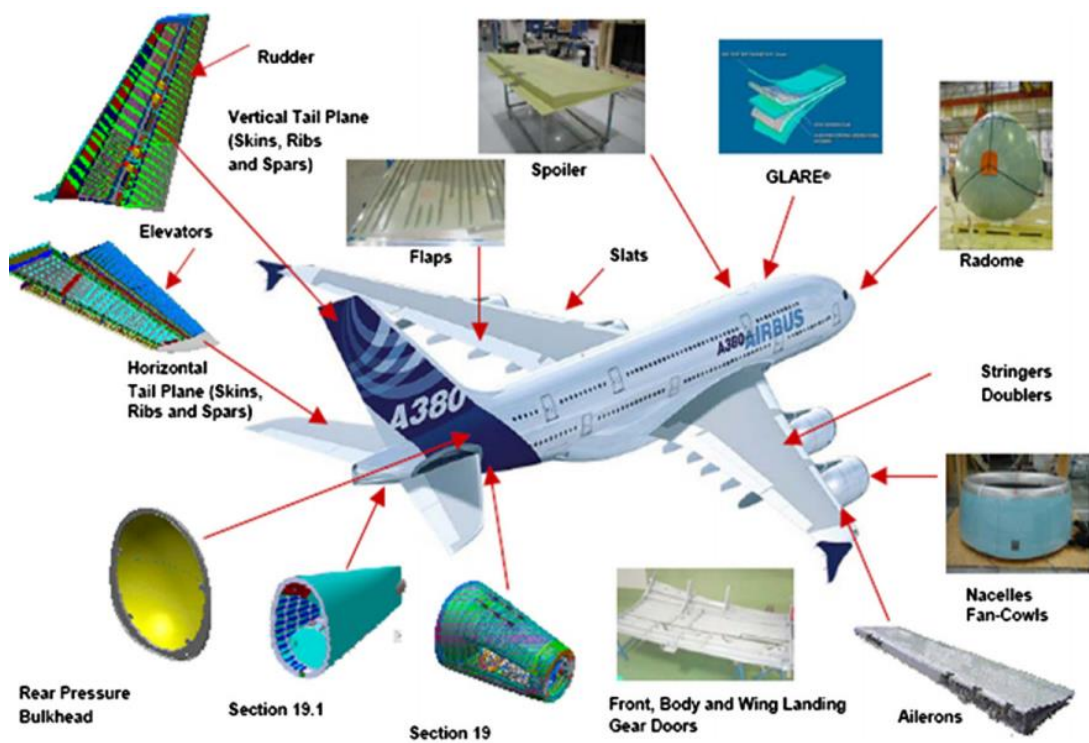


Figure 1-2 Schematic view of the Airbus A380 and adhesive bonding used areas[4]

As the structural behavior of the adhesives was well studied and understood, possible application opportunities for adhesives have been emerged. So, new adhesives were developed for specific applications. Currently, one of the most important research areas is the development of adhesives for electronic applications in the aerospace industry, especially for space applications where environmental conditions become predominant. Electronic applications can be listed as below [5]:

- Bonding of surface-mount components
- Wire tracking
- Potting and encapsulating electronic components
- Conformal coating of circuit boards

Adhesives are valuable for electronics because of their electrical and thermal properties, agility and possibility for design flexibility. Conventionally, almost all electronic applications involve joining of components with circuit boards via soldering. However, soldering operation needs high temperatures (up to 400 °C to melt) that can harm the components or circuit boards. Hence, another advantage of adhesives over traditional joining methods is that they do not need high temperature to cure in case of sensitive applications.

For the development of the application specific adhesives, two methods are constructed:

- Chemical synthesis: adhesives are continuously evolving with advances in material and chemical engineering in time. New compositions and formulations are sampled to construct the best adhesive in every aspect.
- Development of composite adhesives: In some aerospace applications, epoxy adhesives are not qualified to service under flight conditions. Then, there occurs a necessity to improve epoxy adhesives. Another way to achieve that goal is adding organic/inorganic particles into epoxy adhesive. By this method, drawbacks of epoxy can be covered by particles' strength. Then, this constructs a stable and strong epoxy composite adhesive.

Composite adhesives are developed to be either electrically conductive or nonconductive adhesives. For the first group, graphite, graphene and carbon nanotube can be used as additives [6,7]. But, the breakdown strength is affected adversely. It is the minimum voltage to cause spark breakdown across the sample whose thickness is known. The breakdown strength is in terms of volt per unit thickness. Since electrical conductivity is gained by the particles' properties, composite adhesive becomes electrically conductive and this can cause problems on electrical components [8]. In the second group, aluminum oxide [9], zinc oxide [10], boron nitride [11] and titanium oxide [12] are widely preferred as additives. Their electrical resistivity values make them useful in most of the electrical applications. In addition, their improvements on physical properties of neat epoxy are observed as enhanced thermal conductivity and lowered coefficient of thermal expansion [13].

Chemical synthesis needs more sophisticated approach than developing composite adhesives. It is more related to field of chemistry science rather. In addition, it requires lots of time and money investment. However, both electronic and aerospace industries prefer the cost effective solutions on their joint operations. On the other hand, development of composite adhesives is a straightforward process to follow. Pre-synthesized and produced commercial epoxy is a good agent to work with. Since chemical synthesis is not the profession of mechanical, aerospace or material engineers, developing composite adhesives method can be implemented by these engineers easily. It can be said that this process is time and cost saving. Also, filler materials are easy to find and affordable to buy. After all, the development of composite adhesives is more appropriate method to use in products for aerospace industry.

In this work, due to time and cost limitations, development of composite adhesives method was used to produce composite adhesives with enhanced thermal and mechanical properties. In order to achieve this goal, a literature survey was carried out to understand the methodology and, its performance, limitations and test methods. Then, findings gathered from survey were examined and evaluated. After

that, applicable test methods, particle materials and specifications were investigated. Moreover, performance enhancements of composite adhesive structure were collected from literature as well, and they were presented in Literature Survey chapter. Then, necessary tests for the thermal and mechanical properties from literature survey were described in the Test Methods chapter. In the Materials and Preparation Methods chapter, selected particles, particles sizes and geometries were mentioned. Also, sample preparation methods and the points where the attention should be paid were described. Finally, all study outputs were discussed and conclusion remarks were presented.

CHAPTER 2

LITERATURE SURVEY

The need for superior adhesives leads to various studies to focus on developing new materials. On the other hand, strengthening of readily available adhesives is a method on which anyone can work. In aerospace applications, all systems are generally exposed to harsh thermal cycles in flight. Even if adhesives are not expected to bear high stresses; they need to preserve their structural integrity over thermal cycles. Therefore, enhanced thermal properties of adhesives are needed to be achieved by producing composite adhesives.

Among additive particle candidates, hexagonal boron nitride (hBN) has the comparably high thermal conductivity value as ~ 300 W/m.K. Also, it has a low coefficient of thermal expansion value, low dielectric constant, high electrical resistivity and stable crystal structure. Moreover, it has no side effect on neat epoxy's electrical properties [14,15].

Zhou et al. [16] used 0.5 μm sized hBN and diglycidylether of bisphenol A (DGEBA) type epoxy resin in their study. They firstly modified particles' surface with trimethoxysilane and added the filler material in different weight ratios to epoxy resin (0-50 wt. %). Then, for the characterization, Fourier Transform infrared spectrometer (FTIR), differential scanning calorimetry (DSC), thermogravimetric analyzer (TGA), scanning electron microscope, hot disk thermal analyzer and broadband dielectric spectrometer were used. Epoxy initially had a thermal conductivity of 0.22 W/m K. It is stated that adding hBN increases the thermal conductivity values up to 1.2-1.34 W/m K. In Figure 2-1, change in behavior of thermal conductivity can be seen.

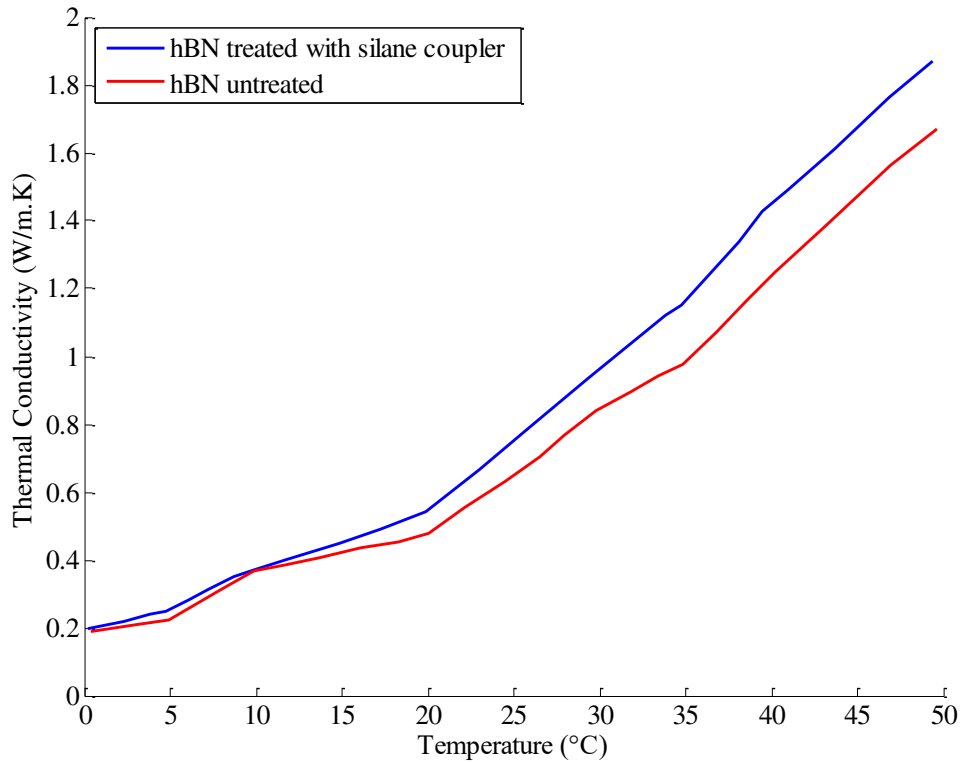


Figure 2-1 Thermal Conductivity Values with increasing hBN ratio [16].

Glass transition temperature (T_g) is a threshold for polymers such that mechanical behavior of polymer is turned from glassy behavior to rubbery. In DSC test results; there is a slight influence on the thermal stability behavior of the composite until filler ratio of 40 wt%. Then, between filler ratios of 40 and 50 wt%, T_g values decreased. T_g in polymers is affected by many factors like free volume and molecular weight [17]. When T_g value is reached, structural integrity of composite adhesive is broken. In Figure 2-2, DSC results of samples can be seen.

For the mechanical tests, samples were prepared in a glass mold. Then, tensile and flexural measurements were performed according to ASTM D-638 and D-790. Also, they measured the impact strength with pendulum impact tester according to ASTM D-256. The effect of hBN filling can be seen in Table 2-1.

Table 2-1 Mechanical Properties of hBN filled Epoxy

Mechanical Properties	hBN Concentration (wt%)				
	0	20	30	40	50
Tensile Strength (MPa)	68.2	63.6	58.2	51.2	45.1
Tensile Modulus (GPa)	2.68	2.82	2.93	3.12	3.14
Flexural Strength (MPa)	112	108	95	86	81
Flexural Modulus (GPa)	2.71	2.79	2.88	3.05	3.07
Impact Strength (kJ/m ²)	16.2	14.5	12.3	10.3	8.2

hBN particles have higher rigidity than epoxy matrix. So, as they are added, both flexural and tensile modulus increased. With increasing hBN content, the viscosity of composite structure began to increase quickly. Therefore, some gaps, interfacial defects and poor wettability between particles and epoxy matrix might occur, resulting in worsening of mechanical properties. Also, a decrease in the impact strength is observed. The filler makes composite structure more viscous than neat epoxy. Then, some voids or internal defects in composite structure may become inevitable. The authors stated that these defects can also affect the mechanical property of composite structure.

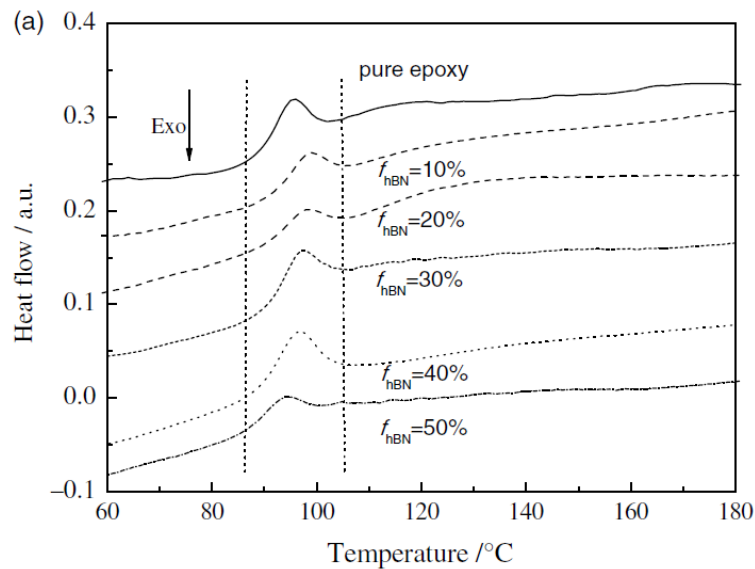


Figure 2-2 DSC Results with varying hBN ratio[16]

Ekrem et al. [18] used boron nitride and carbon nanotube as filler material. They focused on thermal stability and adhesive strength of composite structure. The DGEBA based epoxy was selected as epoxy matrix which was used in defense industry. Boron nitride particles were produced by themselves. They used the arc discharge method for production. Also, carbon nanotubes ($\varnothing 50 \times 10\text{-}30$ nm) were purchased from the market. Adherends were chosen as AL2024-T3 sheets in size of $101.6 \times 25.4 \times 2$ mm. The bonding length was 12.7 ± 0.1 mm. Moreover, six cases were prepared for characterization process. These cases are summarized in Table 2-2. For the thermal analysis, DSC tests and TGA tests were conducted. Single lap strength joint testing was conducted to determine adhesive strength as mechanical property. Test was in accordance with ASTM D1002-10 standard.

Table 2-2 Test Specimens Composition

Case	Carbon Nanotube wt%	Boron Nitride wt%	Epoxy wt%
1	0	0	100
2	0.3	0	99.7
3	0	0.5	99.5
4	0.1	0.5	99.4
5	0.3	0.5	99.2
6	0.5	0.5	99

It can be concluded from the results that filler materials had improving effect on mechanical property of epoxy adhesive [18]. Nanoparticles and epoxy have an intimate contact. Then, particles fill the pores in the epoxy structure and improve the strength of bond. This mechanism is described by mechanical interlocking [19]. Their measurements showed that neat epoxy had approximately 10 MPa shear strength. Case 3 had 13 MPa of shear strength which can be stated as slight increase. On the other hand, case 5's shear strength was 15 MPa. So, the synergetic effect of these two fillers is more effective than single filler type. Slight increase can be explained by agglomeration and/or wetting problem.

Improvement of the neat epoxy's mechanical properties by using Al_2O_3 particles has been studied well in recent years [20-24]. Al_2O_3 particles have high stiffness around

386 GPa which is way higher than most of epoxy adhesives. So, there is a huge potential to have well stiffened composite adhesives [25]. Also, they have low density and high dielectric strength which make Al_2O_3 an attractive candidate as additive particle [26].

Jiang et al. [27] studied thermo-mechanical behaviors of reinforced epoxy resins. They used 80 nm Al_2O_3 particles and DGEBA type epoxy resin. The Al_2O_3 weight content is varied from 1 to 4%. In their study, Scanning Electron Microscope (SEM), DSC, TGA, Dynamic Mechanical Analysis (DMA) and Thermal Mechanical Analysis (TMA) were conducted.

In Figure 2-3, DSC results for all samples can be found. Therefore, it can be seen that T_g values are raised from 170 °C to 181.8 °C by increasing weight ratio of Al_2O_3 to 2 wt.%. When filler materials are added into epoxy matrix, particles form bond with polymer chains. Then, these bonds behave in a way to hold polymer chains and particles together. So, glass transition temperatures are increased.

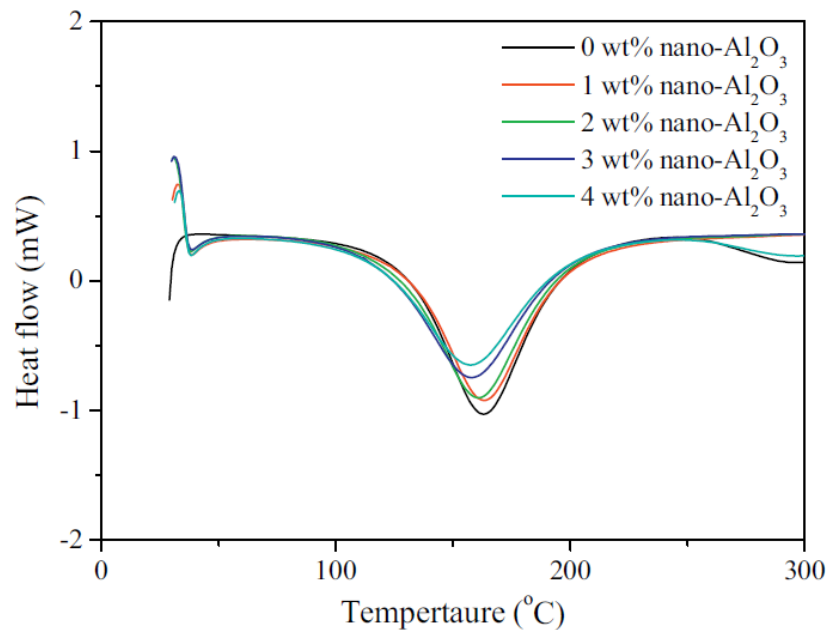


Figure 2-3 T_g Values from DSC Results with varying Al_2O_3 Content[25]

In TGA thermograms, thermal stability of the composite structure can be examined. $T_{5\%}$ values by adding Al_2O_3 are listed in Table 2-3. $T_{5\%}$ is the temperature value where composite structure lost 5% of its weight. In addition, char is the residue from composite structure when it is heated up to 800°C . It can be clearly shown that with particle addition, temperature values remain almost the same as the neat epoxy. So, particle addition has no significant influence on thermal stability of neat epoxy resin. Hence, Al_2O_3 can be approved as attractive candidate by these results.

Table 2-3 Thermal Stability of Composite Adhesive

Al_2O_3 Content (wt%)	$T_{5\%}$ ($^\circ\text{C}$)	Char (%) at 800°C
0	362.1	14.3
1	361.0	15.3
2	360.8	16.5
3	361.0	17.5
4	358.2	18.2

It can be seen from TMA results that there is a decreasing trend in coefficient of thermal expansion (CTE) over increasing the Al_2O_3 . In glassy region, CTE values decreased from 79.8 to $75.5 \times 10^{-6} \text{ } 1/^\circ\text{C}$. Moreover, storage modulus decreased from 1513 to 1378 MPa. On the contrary, in rubbery region, it increased from 37.7 to 41.4 MPa. Therefore, these composite adhesives have good heat resistance with increased particle percentage [27]. In addition, Hu et al. [28] focused on production of Al_2O_3 particles which have promising synergy with epoxy adhesive for electronic packaging. They produced 1.36 μm sized Al_2O_3 particles. Also, they compared its performance with aluminum nitride, silicon dioxide and diamond particles in the literature. Composite adhesives with 58 and 70 wt% filler content were produced. Result of samples with 60 wt% Al_2O_3 filler content was compared with their own composite adhesives. For the characterization of composite, field emission scanning electron microscope (FESEM) observations, TGA, thermal conductivity, dielectric

measurement and flexural strength measurements are done. In Figure 2-4, it can be seen that the thermal conductivity value is increased from 7.15 to 13.46 W/m K over 58% to 70% Al_2O_3 content. The sample whose results were taken from literature had the thermal conductivity of 4.3 W/m.K. The filler material prepared by Hu et al. had brilliant effect on thermal conductivity compared with commercial Al_2O_3 particles.

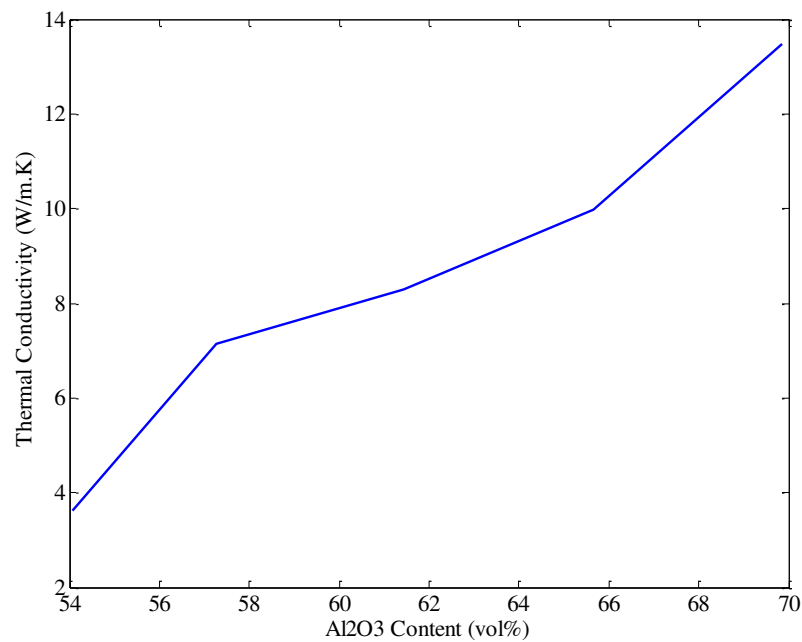


Figure 2-4 Thermal Conductivity over Al_2O_3 Content[26]

Flexural strength tests showed that adding Al_2O_3 had constructive effects on flexural strength. It is measured as 150.9 MPa for 58 wt% Al_2O_3 content. Then, for 70wt% Al_2O_3 content, it is increased to 305 MPa. In addition, dielectric constant is also raised from 6.4 to 7.6 kV/mm [29].

Zhai et al. [30] also used nano- Al_2O_3 as filler material to produce a composite adhesive structure with better thermal, mechanical and multifunctional properties. Their work focused on adhesion strength of epoxy adhesive. The nano- Al_2O_3 particles were in average size of 80nm diameter. Then, as an epoxy adhesive, commercially available two component epoxy was selected. The adhesion strength

was measured by pull-off adhesion test. Test method was in accordance with the standards of ASTM D4541 and ISO 4624. Steel dollies in 20 mm diameters and steel sheets in 100x40x1.7 mm were used as adherends. They prepared neat epoxy and 2wt% Al_2O_3 samples and three different steel sheets with different surface roughness. So, they also tried to explain the relationship between adhesion strength and surface treatment of adherends. Test results showed that nano- Al_2O_3 had significant influence on adhesion. Adding 2 wt% nano- Al_2O_3 increased the neat epoxy's adhesion strength from 3.8 to 18.4 MPa. In addition, surface abraded with 150 grits silicon carbide paper had this best strength.

Bian et al. [14] studied the synergistic effects of the micro-BN and nano- Al_2O_3 added composites. As an epoxy resin, DGBEA type is selected. Micro-BN particles are in $\sim 10\mu\text{m}$ size and nano- Al_2O_3 particles are in $\sim 30\text{nm}$ size. In order to examine the effects of filler arrangement, they prepared and labeled composite specimens as BdAKx-y/z where Bd is modified BN, AK is modified Al_2O_3 , x is total filler content in wt. %, y/z represents Bd/AK proportion in total filler content. Their tested composite specimens are shown in Table 2-4.

Table 2-4 Test Specimen Matrix

BdAKx-y/z																
x	0	10					20					30				
y	N/A	0	1	2	3	4	0	1	2	3	4	0	1	2	3	4
z	N/A	4	3	2	1	0	4	3	2	1	0	4	3	2	1	0

SEM, DSC, TGA and dielectric measurement are done for characterization. T_g value of neat epoxy resin is measured as 133.22°C . Then, for the same y/z ratio with increasing x value, T_g values are in lowering trend. For Bd/AK10-3/1 to Bd/AK30-3/1, T_g value is decreased to 126.75°C . In addition, for 30 wt% filler content, there is no distinctive behavior in changing of T_g value with different y/z ratios. This can be explained by that there should be an interface compatibility problem between the

filler and matrix which is inevitable. Consequently, there occur tiny gaps and defects that have effect on chemical behavior of composite adhesive. Thermal conductivity values tend to increase with both x and y/z values. The neat epoxy's thermal conductivity value is measured as 0.169 W/m.K. Increase in y/z has greater influence on thermal conductivity. For instance, samples with x value as 30 have following thermal conductivity values over y/z values 0/4, 1/3, 2/2 and 3/1; 0.373, 0.542, 0.822 and 1.182 W/m.K. For the dielectric constant, filler materials have positive effect on it. Since Al_2O_3 has better dielectric properties, increasing Al_2O_3 partition enhances dielectric constant more than BN particles. In their work, they did not conduct tests to characterize mechanical properties.

Titanium oxide particles are characterized by good chemical stability, high chemical resistance and high hardness [31]. In recent years, titanium oxide particles' effects on the properties of neat epoxy adhesive have been studied. These studies showed that addition of titanium oxide particles increases the flexural strength, elastic modulus and crack resistance [31,32]. In addition, significant improvements in thermal and viscoelastic properties of the neat epoxy resin are seen in the literature by addition of titanium oxide particles [33]. TiO_2 particles have impressive reactivity with epoxy matrix, so it can be expected that they have favorable influence on mechanical properties of composite structure.

Sahu and Satapathy [34] held a study on micro-sized titanium oxide added epoxy resin to enhance thermal conductivity of composite adhesive. Their work was focused on microelectronic applications. Technological developments on microelectronics lead to demands in faster and denser circuits. So, avoiding overheating of the components was highly required. In their work, they also proposed effective thermal conductivity correlation to eliminate testing procedure. In addition, they calculated the effective thermal conductivity values by different methods like Maxwell's method and Lewis Nelson's Method. As epoxy resin, they used one of the commercially available DGEBA type epoxy. The neat epoxy had thermal conductivity value of 0.363 W/m K. For the additive particle, 100 μm sized

titanium oxide (TiO₂) was procured for its moderate density which was 4.197 g/cc. Moreover, particles had the thermal conductivity value of 11.6 W/m K which is relatively high when compared to epoxy itself. They prepared 11 samples with varying TiO₂ from 0 to 25 vol%. Measured thermal conductivity values can be seen in Table 2-5.

Table 2-5 Thermal Conductivity Values of TiO₂ added Composite Adhesives

Filler Content (vol%)	Measured Thermal Conductivity (W/m K)
0	0.363
2.5	0.364
5.0	0.398
7.5	0.417
10.0	0.469
12.5	0.520
15.0	0.581
17.5	0.632
20.0	1.108
22.5	1.117
25.0	1.120

Kumar et al. [35] focused on improvement of mechanical and thermal properties in their study. They used one of the commercially available DGEBA type epoxy resin. Also, 30-40 nm sized TiO₂ with purity of 99.9% is selected as the additive particle material. Three types of samples were prepared by ratios of 5, 10 and 15 wt%. In order to observe changes in thermal properties, DMA and TGA tests were conducted. Hence, up to 10 wt%, storage modulus is increased. But, at 15 wt%, it is suddenly decreased. This decrease is due to the fact that by increasing the movement of chains and molecular motion, storage modulus tends to decrease. Since, polymer chains move instead of standing still and storing energy under deformation. In the study, it was seen that agglomeration and density was increased at 15 wt%. Then, agglomeration seemed suspicious reason for this drop in storage modulus. From DMA results, in the glassy region, enhancement of 29% of storage modulus was obtained at 10 wt%. In addition, thermograms from TGA tests showed that up to 10 wt% thermal stability was increased. But, at 15 wt%, it was dropped.

Table 2-6 TGA Values for Thermal Stability

Weight Loss (%)	Decomposition Temperature (°C)			
	Neat Epoxy	5 wt%	10 wt%	15 wt%
25	371	374	378	375
50	381	388	393	389
75	401	415	435	420

Tutunchi et al. [36] studied on adhesion strength of steel-glass/epoxy composite joints. In their work, two-part structural acrylic adhesive and nano-TiO₂ were included. In addition, as usual, adhesive were selected among commercially available ones. Nano-TiO₂ particles were in size of 20 nm diameter. Composite structure was prepared in 8 different types for 8 different composition of epoxy/filler material. These compositions were listed as; 0, 0.5, 1.0, 1.5, 2.0, 2.5, 3.0 and 3.5 wt% ratio of nano-TiO₂ to epoxy. Then, the samples were characterized by shear, tensile and peel tests. Peel tests were prepared as T-peel (90°) and test was conducted in accordance with standard of ASTM D1876-08. For tensile tests, tensile butt joints were arranged and tested according to standard of ASTM D2095-96. Then, single lap shear joints were assembled and test was managed in accordance with standard of ASTM D1002-10. From tensile and shear test results, it could be said that up to 3wt% adding TiO₂ increased the adhesion strength. Summarized results are tabulated in Table 2-7.

Table 2-7 Test Results of Samples

Composition (wt%)	Shear Strength (MPa)	Tensile Strength (MPa)	Peel Strength (N/mm)
0	22.6	27.0	47.5
0.5	23.2	27.2	36.0
1.0	27.0	30.0	27.0
1.5	28.5	31.1	27.1
2.0	29.0	35.2	36.5
2.5	30.0	37.5	39.5
3.0	33.2	43.0	35.0
3.5	27.1	38.0	34.7

Improving the adhesion strength was highly affected by stress transfer between epoxy matrix and particles. Enhancement in strengths can simply be explained

phenomenon. As mentioned before, these particles and epoxy matrix were in intimate contact [19]. This contact made stress transfer efficiently onto joined particles. Therefore, higher joint stresses were achieved. Weakening of strengths after 3 wt% TiO_2 could be explained that all particles filled gaps in epoxy matrix and made intimate contact with epoxy. So, further added particles could not interact effectively and made epoxy matrix poor. Also, viscosity of composite structure was increased by adding particles which could lead to non-uniform distribution of TiO_2 into epoxy matrix. Moreover, because of high viscosity, problems in degassing could be occurred. Therefore, mechanical behavior of epoxy matrix was diluted.

Titanium oxide with Au-doped (TiO_2+Au) was synthesized at the material laboratory at Christian-Albert University. Hierarchical Au Needle Clusters (HAuNCs) were accumulated on TiO_2 particles by the photocatalytic reduction of Au^{3+} ions. Then, TiO_2 particles were plunged into a quartz cuvette filled with aqueous HAuCl_4 solution. Later, UV LED with wavelength of 365 nm irradiated the quartz cuvette. After irradiation process, the particles were rinsed with deionized water and dried with nitrogen [37]. There is no literature information about usage of TiO_2+Au as filler material in composite structure. Also, there is lack of mechanical and thermal properties as expected. TiO_2+Au particles and epoxy interaction is illustrated in Figure 2-5. Since TiO_2 particles have better reactivity with epoxy, OH bonds are constructed between TiO_2 particles and epoxy matrix which are illustrated as green arrows. On the other hand, Au particles are not willing to construct bonds with epoxy matrix which are illustrated as red arrows. Also, Au particles have poor mechanical properties by contrast with their excellent thermal properties. With the TiO_2+Au and epoxy combination, mechanical properties of TiO_2 and thermal properties of Au are fused together to have enhanced filler material.

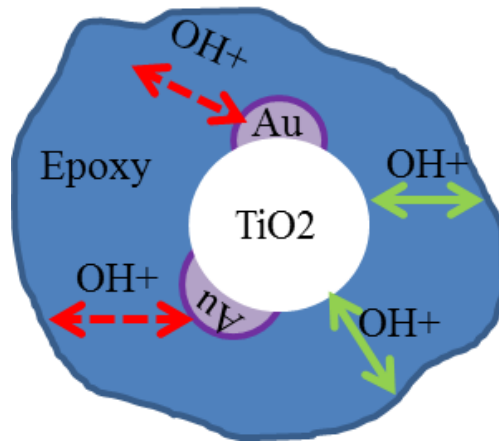


Figure 2-5 TiO₂+Au and Epoxy Interaction

2.1. Aim of the Study

With the development in the fields of chemistry and material engineering, adhesives take more places in the aerospace industry. In the aerospace industry, performance criteria become more compelling. In this thesis, the development and characterization of composite adhesives were conducted for a special case study.

In this case study, the research was focused on an application where adhesives are used to join glass to metal and glass to glass parts. Also, relative positions of these parts are important to fulfill operation requirements. For this assembly, service temperature is determined to be between -30 to 55 C°. Used adhesive is a commercially available epoxy adhesive, Loctite 9412. Its thermal properties are insufficient to endure heat cycles. Therefore, structural integrity failed due to the lack of heat conduction. As a result, assembly is no more operable. Then, it can be seen that there should be more sophisticated adhesives to fulfill this industry's needs. Regarding this, development of composite adhesives is adopted way to enhance thermal properties of commercially available epoxy resin by adding particles. Then, from the literature, hBN, Al₂O₃ and TiO₂ particles become prominent candidates as filler particles. Moreover, Au-doped TiO₂ particles are synthesized due to its expected greater thermal properties for this study as filler particles. In order to

characterize the thermal properties of composite adhesive, following tests are conducted in accordance with literature;

- Dynamic Mechanical Analysis (DMA)
- Differential Scanning Calorimetry (DSC)
- Scanning Electron Microscopy (SEM)
- Thermal Conductivity (TC)
- Fourier Transform Infrared Spectrometry (FTIR)
- Single Lap Shear Test

CHAPTER 3

TEST METHODS

Testing of the samples is the core of this study. In order to have meaningful results, test devices and their working principles should be known well. Also, sample dimensions have an influence on the test results. Therefore, there should not be geometrical difference between samples. Hence, it can be said that test results vary only with sample's internal structure which is the aim of testing.

In this chapter, conducted tests necessary to characterize composite adhesive are described. Used test devices and their working principles are also explained. Moreover, the standards followed during tests and sample geometries are mentioned.

3.1. Dynamic Mechanical Analysis (DMA)

DMA is a widely used technique to characterize sample's mechanical properties over temperature, time, frequency, stress, atmosphere or combination of these parameters. In DMA technique, sinusoidal small stress is applied to the sample. Then, response of sample is read by the DMA device. Therefore, stiffness and damping are measured. The stiffness is separated in two parts; storage modulus and loss modulus. Since the excitation is in sinusoidal form, storage modulus (E') is the in-phase component of stiffness which is a measure of elastic response of material. Also, it is related with the stored energy in polymer. The loss modulus (E'') is the out of phase component which is a measure of viscous response. It is related with energy dissipation as heat. These are reported as damping and modulus. Damping is the energy dissipation of material in cyclic loading. It is also the ratio of loss to storage modulus which is called as $\tan\delta$ and equated by following equation;

$$\tan\delta = \frac{E'}{E''}$$

ARES G2 Rheometer was used for DMA tests in torsion mode which is shown in Figure 3-1. Samples were prepared in dimensions of 4 x 10 x 50 mm and heated from 25 to 250 °C with 5 °C/min at frequency of 1 Hz. Tests are conducted in accordance with ASTM D 7028 standard. The tolerance in the results is 8%. The example of prepared samples can be seen in Figure 3-2.



Figure 3-1 ARES G2 Rheometer (<https://www.tainstruments.com/ares-g2/>)



Figure 3-2 DMA Sample

3.2. Differential Scanning Calorimetry (DSC)

The DSC is a well-known technique in thermal analysis. Simply, this device is used to see how polymers' thermal behavior changes when heat is applied. There are two heating pans. The sample is placed in the one pan and the other one is left empty. Later, the device heats the both pan with same heating rate. As expected, the pan with sample is needed to be heated more. Then, it can be made that a plot of difference in heat output over temperature. In addition, the device can detect the phase transitions of the sample like glass transition, crystallization and melting. In the plot, after a certain temperature, curve is shifted upward suddenly. This certain temperature is named as glass transition temperature. In Figure 3-3, an example plot of heat flow over temperature can be seen. The sudden change in curve is pointed on the plot and the temperature where it occurs is the glass transition temperature. TA Instruments Q200 model is used for DSC analysis seen in Figure 3-4. The test environment is He or N₂ atmosphere. Samples were prepared with the dimensions of Ø10x10 mm which can be seen in Figure 3-5. Then, they were heated at rate of 10 °C/min. Gas is flowing at 25 mL/min. The tolerance in measurements is ±3 °C. The tests were conducted in accordance with following standards;

- ASTM E 1269 – 01,
- ASTM E 1356 – 03,
- ASTM D 3418-03,
- ISO 11358,
- ASTM E793,
- ASTM E 698

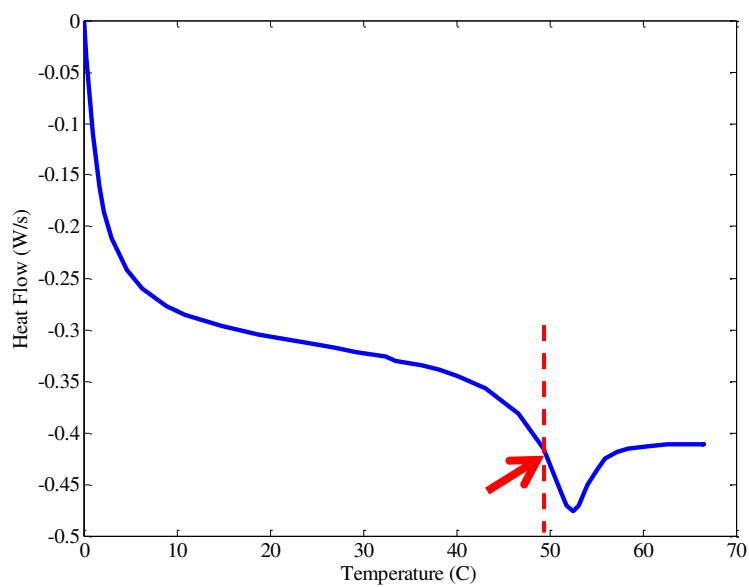


Figure 3-3 Example of DSC Plot



Figure 3-4 TA Instruments Q200 (yorku.ca/tbaumgar/photo/album/ta-instruments-dsc-q200)



Figure 3-5 DSC Sample

3.3. Fourier Transform Infrared Spectrometer (FTIR)

Fourier Transform Infrared Spectrometer (FTIR) is an analytical method which is widely used in academic laboratories and industrial applications. It aims to understand the internal structure of materials and composition of molecular mixtures. Also, identification of bonds between organic/inorganic molecules is intended in this method. FTIR spectroscopy uses radiation which is modulated and mid-infrared to interrogate the sample. The radiation is absorbed by sample at specific frequencies. Also, these frequency values are related to vibrational bond energies of functional groups in the sample. Hence, the device measures the absorbed partition of this radiation and plots transmittance versus wavelength as an output. The bands where absorption occurs can be used to diagnose molecular components and structures. Higher vibrational state is reached by molecules after they absorb the radiation. The wavelength of light absorbed is a function of energy absorption and unique for every molecule. Bruker Tensor 27 is used to perform this measurement which can be seen in Figure 3-6. This device's range of wavelength is between $400 - 4000 \text{ cm}^{-1}$ and resolution is 1 cm^{-1} . In the range of $4000-1500 \text{ cm}^{-1}$, absorption is due to functional groups e.g., $-\text{OH}$, $\text{C}=\text{O}$, $\text{N}-\text{H}$ etc. But, the region from $1500-400 \text{ cm}^{-1}$ is where the material specific absorption bands are occurred. The

sample is the one used in DMA tests. The measurements were performed in accordance with ASTM E1252 standard.

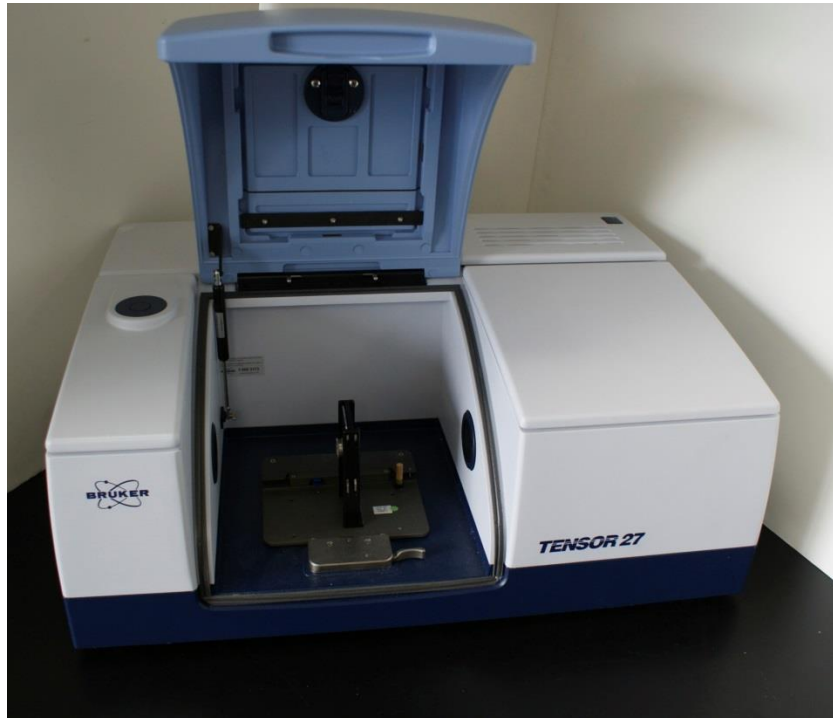


Figure 3-6 Bruker Tensor 27 FTIR Spectrometer(<http://triadsci.com/en/products/ftir-ir-and-near-ir-spectroscopy/946/bruker-tensor-27-ftir-bruker-ftir-bruker-27/251160>)

3.4. Thermal Conductivity (TC)

Thermal conductivity is described as ability of materials to conduct heat through itself. Thermal conductivity is one of the crucial properties for the materials under service where high temperature gradients occur. The sample is placed and compressed with a load between two plates in the device. The lower plate is also connected to a heat flux transducer which is calibrated. When heat is transferred from upper plate to lower plate, a temperature gradient is built across sample. This temperature gradient and heat transfer are measured by the device. With the known thickness, thermal conductivity can be calculated for the sample. TA Instruments DTC-300 shown in Figure 3-7 is used. The sample has dimensions of Ø50x6 mm which can be seen in Figure 3-8. The tests were conducted in accordance with ASTM E1530 standard.



Figure 3-7 TA Instruments DTC-300 (<https://www.tainstruments.com/dtc-300/>)



Figure 3-8 Thermal Conductivity Sample

3.5. Scanning Electron Microscope (SEM)

Scanning electron microscope (SEM) is a type of microscope which is used to study the surface of solid objects. It scans with a focused beam which has relatively low energy over a surface to create an image of sample surface. Firstly, sample is frozen into liquid nitrogen and broken into two pieces. Later, the image is taken from newly

formed broken surface. This image gives information about the sample's inner topography and composition. Carl Zeiss Supra 55 is used for the test, which can be seen in Figure 3-9.



Figure 3-9 Carl Zeiss Supra 55(<https://www.cecni.res.in/SAIF/carl.html>)

3.6. Single Lap Shear Test

Single lap shear strength is a common property available in data sheet of the adhesive. The single lap shear test is also named as thin lap shear test and conducted to measure shear strength of the adhesive film. The test is applied to determine adhesive strength, surface preparation parameters and environmental durability. It is the most extensively method of displaying data on adhesively bonded joints. There are lots of single lap joint shear tests. Test is performed using standard tension/compression mechanical test machine (Instron 5500R) according to ASTM D1002-10 standard which specifies lap shear test for metal to metal specimens. The

device can be seen in Figure 3-10. The pulling rate is 1.3mm/min. The adherends have the dimension of 25.4x101.6x1.62 mm. Examples of test specimens can be seen in Figure 3-11.



Figure 3-10 Instron 5500R

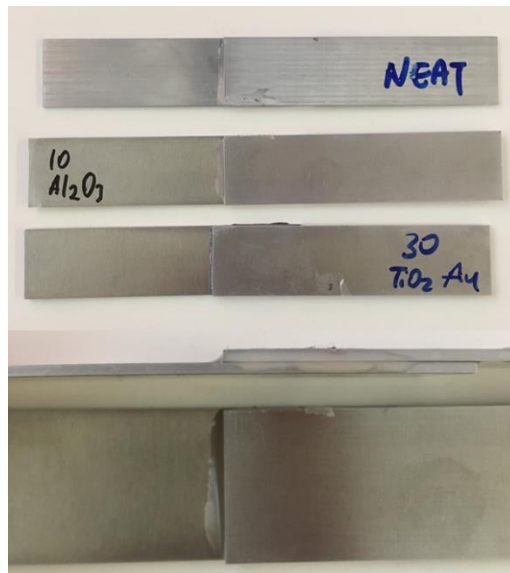


Figure 3-11 Test Samples

CHAPTER 4

MATERIALS AND PREPARATION METHODS

In the aerospace industry, demand for advanced adhesives is increasing. Both strict requirements and scarcity of sophisticated adhesives cause obstacles to fulfill performance requirements. So, development of advanced composite structures using readily available materials become inevitable. These materials including epoxy resin and filler particles can be purchased in large amounts and stocked easily. Therefore, epoxy adhesive is selected due to its easy accessibility. On the other hand, filler particles are the materials which are widely used in previously reported studies. In addition, hBN particles were purchased from Nanografi which is a domestic firm. Moreover, Al_2O_3 particles were from Sigma-Aldrich®. Exceptionally, Au doped TiO_2 particles were synthesized at the material laboratory. The aim of including these particles is the great thermal properties of Au and their acceptable reactivity with TiO_2 particles.

Samples need a well-defined, labor intensive preparation method. For instance, epoxy adhesives have high surface tension which prevents wetting sometimes. This wetting problem results in gaps between particles and epoxy resin and thermal conduction in the composite structure is interrupted. Therefore, adding particles can harm the epoxy adhesive rather than enhancing it. Moreover, the epoxy adhesive is a viscous fluid in most cases. By adding particles, viscosity is also increased. So, pouring into molds becomes a challenging process. Consequently, air bubbles can be trapped easily in this viscous composite structure. Bubbles can cause obstacle in thermal conduction and weakness in mechanical strength. The bubbles in composite structure can be seen in Figure 4-1. This bubbled sample is prepared without a delicate procedure. The enhancement in properties demands also homogeneity in the composite structure. In order to prevent defects and encourage interactions, detailed

sample preparation method is studied and described. In Figure 4-1, a sample without this procedure and one with it can be seen. Therefore, how this method could improve the sample's quality can be seen easily.



Figure 4-1 Bubbled and Regular Samples

4.1. Materials

In this study, commercially available Loctite® EA 9412 Hysol was used. It is a two-part epoxy adhesive with low viscosity. Moreover, its availability and wide usage area in the company make it a strong candidate for epoxy resin in this study. As additive particles, following materials are used; hBN (65-75 nm), Al_2O_3 (80 nm), TiO_2 (~100nm) and Au-doped TiO_2 (~100nm). hBN and Al_2O_3 particles are commonly used additive materials found in literature. TiO_2 particles also occur in literature as additive materials, but not commonly as former ones. Since Au-doped TiO_2 particles are product of a material laboratory, there is no literature knowledge about usage of these particles as additive materials.

4.2. Sample Preparation Methods

Sample preparation has three minor steps which are preparation of molds, preparation of particles and preparation of composite structure. Firstly, all molds and adherends are washed with de-ionized water and wiped with dust dry cloth. Then, for all cleaning and degassing steps, ultrasonic cleaner is used as a preliminary step for preparation. The device is one of the Cole-Parmer® ultrasonic cleaners. Before the processes, ultrasonic cleaner is checked and degassed. After ultrasonic cleaning, oven is used for particle drying and curing the composite adhesive. Moreover,

vacuum oven is used in only vacuum mode for de-airing pre-mixture of epoxy resin and particles. Also, supplementary tools are cleaned with de-ionized water, acetone and alcohol. Then, they are visually controlled for any residuals which come from previous samples.

4.2.1. Molds/Adherends Preparation

There are four molds and two adherends to prepare test samples. Firstly, they are dismantled. Then, residue of adhesives on the molds from previous operations are removed gently. All parts are cleaned in ultrasonic cleaner at acetone, ethanol and de-ionized water filled beaker respectively for 20 min each. Afterwards, parts are dried with nitrogen. Finally, all molds are assembled and ready for operation. In Figure 4-2, used molds are illustrated. Molds are manufactured from Teflon material to provide that cured composite adhesive can be removed from molds easily. In addition, the adherends for single lap shear tests are manufactured from Al 2024-T3 in accordance with ASTM B-209 standard.

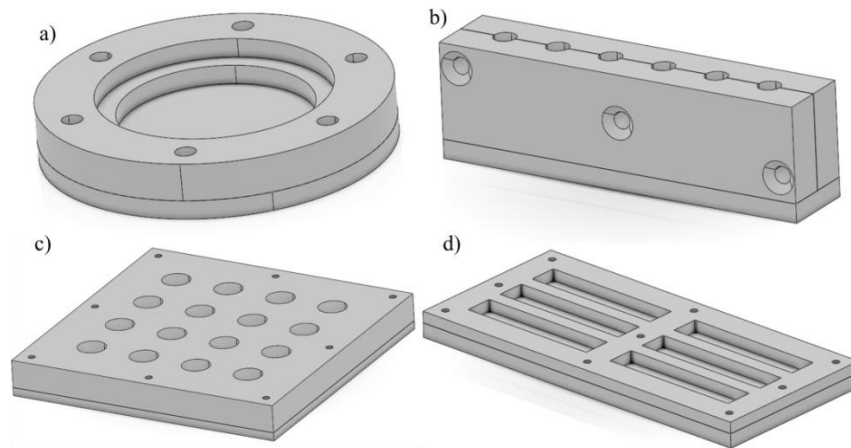


Figure 4-2 Molds of a) Thermal Inductivity b) FT-IR c) DSC d) DMA Tests

4.2.2. Particles Preparation

Humidity on particles is a possible cause for wetting problem between particles and epoxy resin. So, particles are weighed and transferred to ceramic containers. Before mixing, all particles are baked at 120 °C for 1 hour on the purpose of

dehumidification. After baking, ceramic containers are cooled to room temperature. In order to prevent dust or other dirt particles, aluminum folio is used as lid.

4.2.3. Composite Adhesive Preparation

Part A of epoxy adhesive is transferred to Teflon beaker with attention not to cause air bubbles in it. In the vacuum cabinet, adhesive can be spilled out while de-airing. In order to prevent this, as a preliminary de-airing process, the beaker is de-aired in ultrasonic cleaner for 20 min. Then, beaker is vacuumed in vacuum cabinet to 4.2 Torr for 1 hour to de-air completely. Afterwards, de-aired part A and baked particles are mixed together until blend gets homogeneous. Later, mixture is de-aired in ultrasonic cleaner for 20 min and vacuum cabinet for 1 hour as mentioned before. Then, part B is added to blend and mixed to get homogeneous blend. By adding part B, curing process is started and there is a need to operate faster. Final blend is de-aired in ultrasonic cleaner for 2-5 min. Finally, blend is poured into molds. In order to prevent air bubbles, pouring is done carefully, slowly and very close to bottom of molds. The composite adhesive is cured in oven at 82 °C for 1 hour. The method is illustrated in Figure 4-3 for hBN and Al₂O₃ particles.

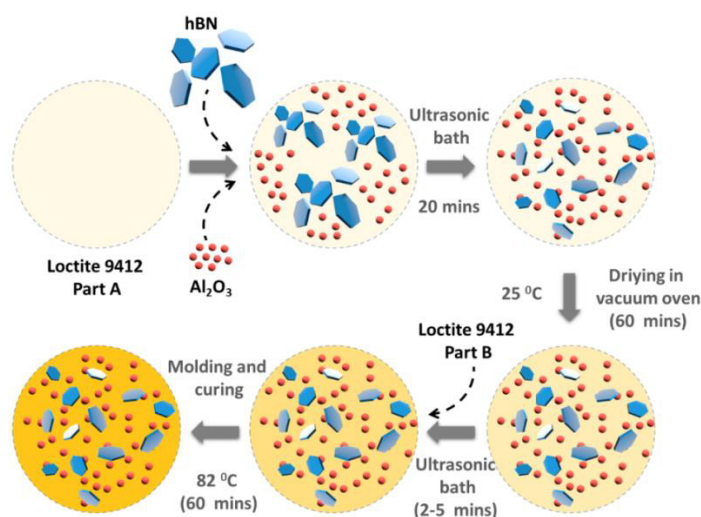


Figure 4-3 Example Schematic Presentation for the Sample Preparation

CHAPTER 5

RESULTS AND DISCUSSION

Samples were prepared in accordance with an exclusive preparation method. Since defects in samples affect test results dramatically, following this method is crucial to produce homogenous and flawless samples. Also, samples were fit for related international standards. By this way, comparison of the test results got from this work and previous studies becomes simpler. In addition, all tests were conducted in conformity with international standards. This also contributes the comparability and reliability of study. The preliminary results of this work are reported and published [38,39].

Composite adhesive's mechanical properties over temperature were measured by DMA tests, namely storage modulus and loss factor. The storage modulus can be related with cross-links between epoxy resin and particles. Moreover, storage modulus of samples can be seen in the following figures.

In Figure 5-1a, improvement effects of adding hBN over neat epoxy can be seen. For the service temperatures less than 55 °C, up to 30 wt% ratio, hBN has no constructive effect on mechanical properties of neat epoxy. On the contrary, 30 wt% ratio of hBN improves the storage modulus but its contribution is less significant. For 20wt% hBN content, storage modulus decreases for all temperature range. As cross-linking increases, storage modulus is expected to increase. Therefore, the decrease in storage modulus might be caused by poor interaction between particles and epoxy. In the light of this information, additional action is necessary to make improvements in mechanical properties. Moreover, in Figure 5-1b, Al₂O₃ particle's development in mechanical properties is shown. In service temperature range, there is a downgrade in storage modulus for 10 wt%. But, after 40 °C, storage modulus becomes higher than neat epoxy. For the 20 wt% ratio, an obvious improvement can be seen thanks to favorable alignment of Al₂O₃ particles into composite adhesive.

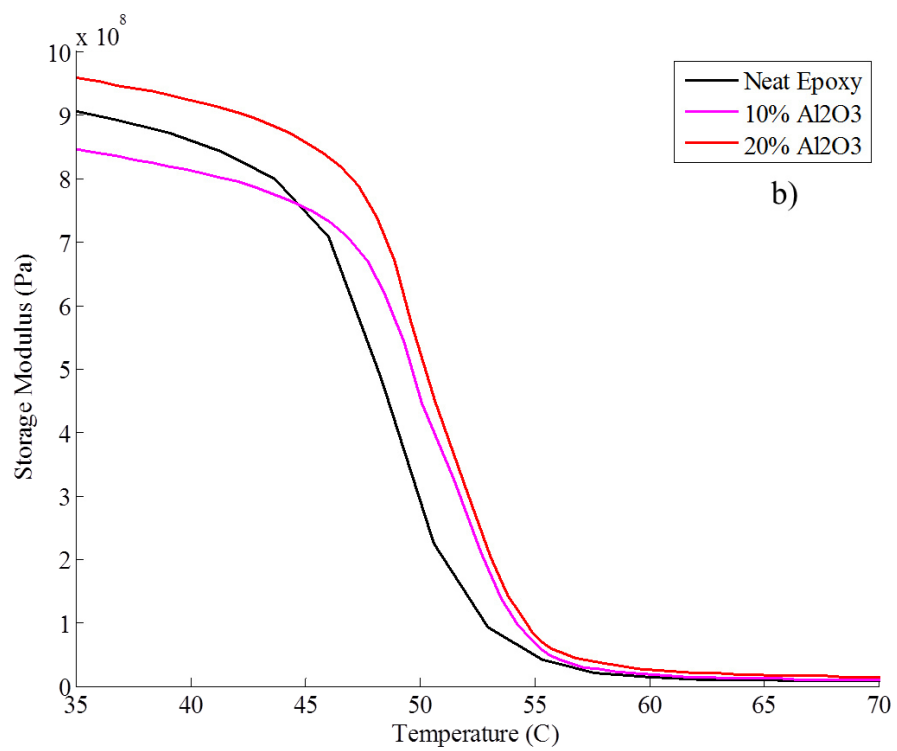
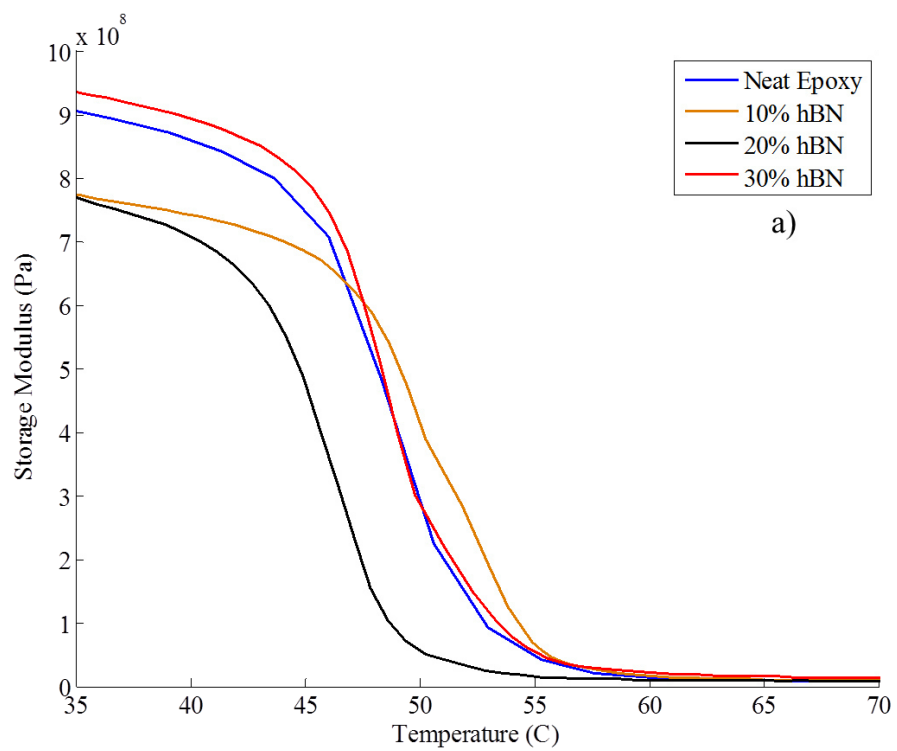


Figure 5-1 a) hBN particle b) Al₂O₃ particle improvement on storage modulus

The loss factor ($\tan \delta$) of samples obtained from DMA can be seen in Figure 5-2. The loss factor is described as ratio of loss modulus to storage modulus. The loss modulus can be stated as the energy dissipation of polymer chain motion in composite adhesive. Except 30wt% TiO_2 and 20wt% hBN, addition of particles shifts the peak position of loss factor. The loss factor also gives an assessment about the composite's damping effect.

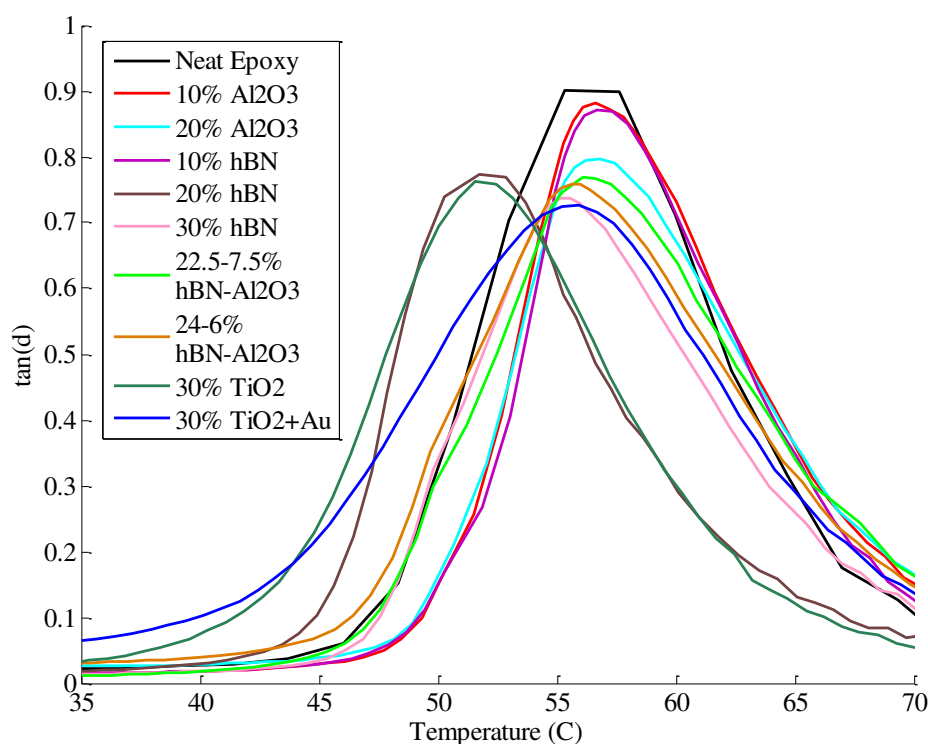


Figure 5-2 Loss Factor of Samples

In Figure 5-3, effect of synergetic mixture of hBN and Al_2O_3 on neat epoxy is considered. Also, effects of TiO_2 and TiO_2+Au can be seen. In Figure 5-3a, 22.5-7.5 wt% hBN- Al_2O_3 particle mix does not upgrade or downgrade the storage modulus. In addition, 24-6 wt% hBN- Al_2O_3 particle mix has improvement in service temperature. Its behavior during glass to rubber transition matches with neat epoxy. Furthermore, in Figure 5-3b, adding TiO_2 or Au doped TiO_2 does not improve the

mechanical properties. Likewise, it worsens the storage modulus in whole service temperature range.

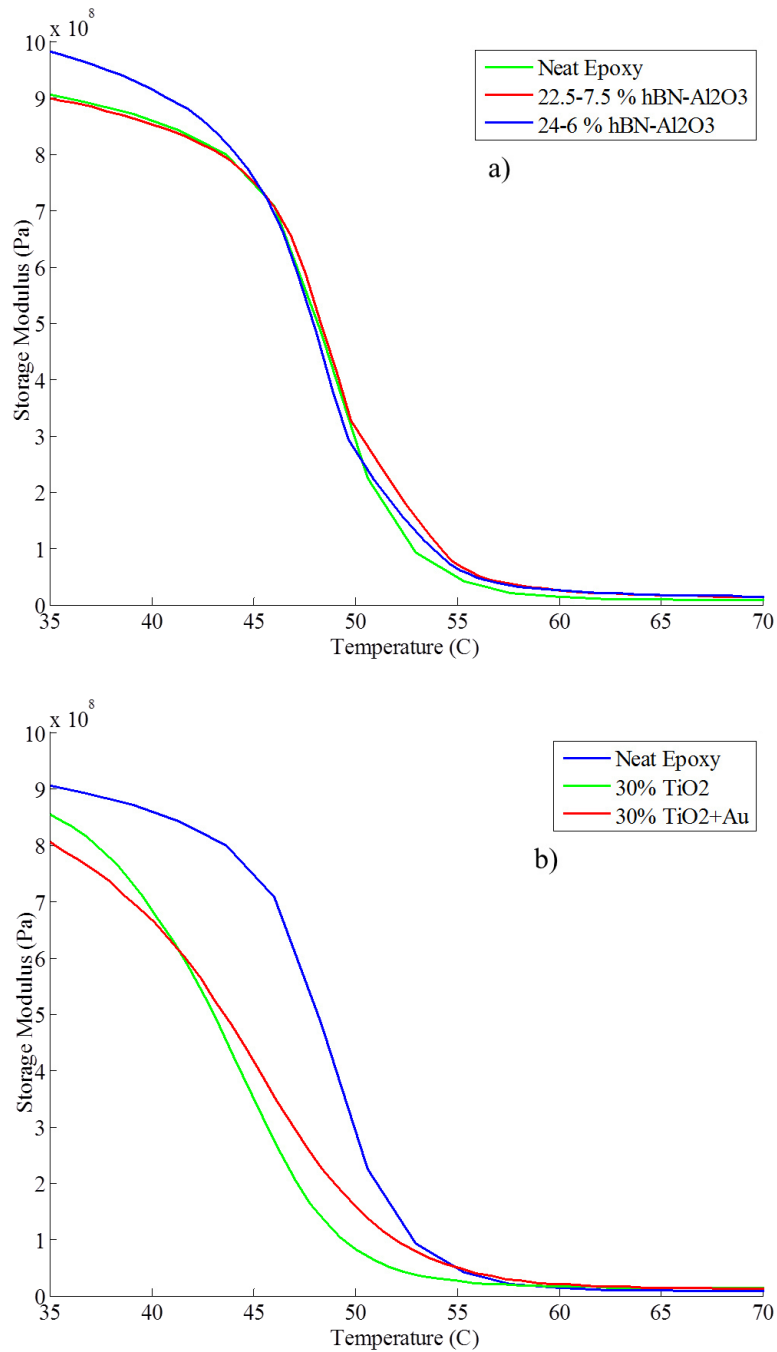


Figure 5-3 a) Synergetic Mixture of hBN-Al₂O₃ b) TiO₂ and TiO₂+Au improvement

Overall comparison of particle addition effects on storage modulus is shown in Figure 5-4. The more favorable improvement is achieved by 24-6 wt% hBN-Al₂O₃ particle mix in the temperature range of 30 to 40 °C. After that region, 20 % Al₂O₃ ratio has better behavior of storage modulus.

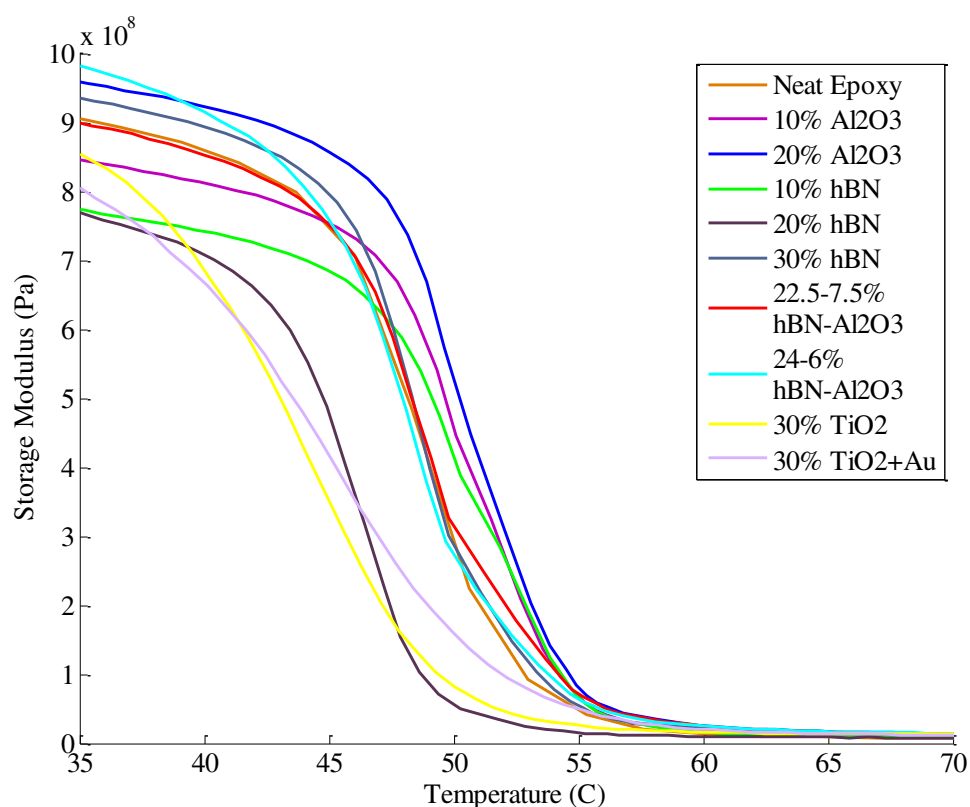


Figure 5-4 Storage modulus over temperature for all samples

DSC tests were conducted to measure glass transition temperature (T_g) value of polymers. In order to achieve this goal, adhesives are needed to be solid and still. After T_g value is reached, adhesives behave like rubbery polymer which is undesirable. In Table 5-1, T_g values of all samples can be found. Al₂O₃ enhances T_g value faster than hBN. In the particle mix configuration, the mix with more Al₂O₃ has better value than other sample. TiO₂ and Au doped TiO₂ particles have the most favorable improvement on T_g value.

Table 5-1 Glass Transition Values of All Samples

Samples	Tg (°C)
Neat Epoxy	44.54
+10% h-BN	45.82
+20% h-BN	47.08
+30% h-BN	49.73
+10% Al ₂ O ₃	47.73
+20% Al ₂ O ₃	47.98
+22.5% h-BN+7.5% Al ₂ O ₃	49.00
+24% hBN+ 6% Al ₂ O ₃	47.04
+30% TiO ₂	51.55
+30% TiO ₂ +Au	55.92

As can be seen in Figure 5-5, added particles form thermal conductive pathway to enhance thermal conductivity of composite adhesive. Adding hBN shows the most significant improvement on neat epoxy's thermal conductivity. This is expected since hBN platelets have relatively high thermal conductivity (~300 W/m.K). Thermal conductivity values at different temperatures are briefed in Table 5-2. It can be easily seen that thermal conduction is carried by hBN platelets mostly. The more hBN it contains, the more heat it can transfer. When concentration of hBN increases, platelets start to contact each other and form a favorable pathway to thermal conduction. This mechanism also works for other type of particles except TiO₂+Au. The thermal conductivity values of synergetic mix of hBN and Al₂O₃ shows that only hBN is not adequate to carry all the heat because of the wetting problem on the

platelets and gaps around platelets. Al_2O_3 has the geometry of sphere. Therefore, it is expected to fill these gaps and make thermal conduction continue.

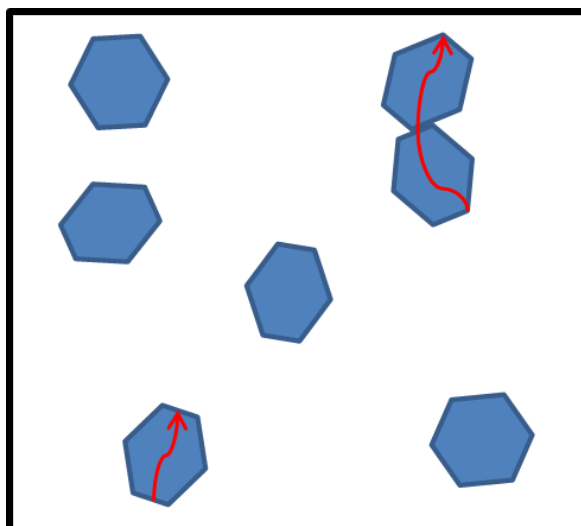


Figure 5-5 Thermal Conductive Pathways in Composite Adhesive Structure

As can be seen in Table 5-2, the sample with higher hBN content has more thermal conductivity value than one with less hBN content. Moreover, TiO_2+Au particles have negative effect on thermal conductivity. As cause for this situation, it is considered that precipitation of Au doped over TiO_2 in the composite structure affects adversely. So, there is a lack of thermal pathways that it should not exist.

Table 5-2 Thermal Conductivity Values (W/m K) of Samples at Different Temperatures

Temperature Ratios		-15 C°	0 C°	20 C°	50 C°	100 C°
Neat Epoxy	-	0.18	0.17	0.18	0.19	0.19
hBN	10 wt%	0.282	0.271	0.244	0.254	0.257
	20 wt%	0.32	0.327	0.295	0.31	0.319
	30 wt%	0.374	0.384	0.359	0.371	0.386
Al_2O_3	10 wt%	0.21	0.207	0.213	0.215	0.213
	20 wt%	0.227	0.231	0.22	0.222	0.219
hBN+ Al_2O_3	22.5-7.5 wt%	0.35	0.347	0.342	0.349	0.352
	24-6 wt%	0.334	0.338	0.328	0.339	0.343
TiO_2	30 wt%	0.247	0.255	0.268	0.28	0.283
TiO_2+Au	30 wt%	0.136	0.144	0.152	0.158	0.174

FTIR spectroscopy is used to analyze chemical composition of substance. Also, characteristic molecules and specific bonds between molecules can be inferred for samples. In the reference spectrum which can be seen in Figure 5-6, expected absorbance of interatomic bonds is given corresponding to the wavenumber. By comparison with this reference spectrum, spectra got from samples are examined. In Figure 5-7, FTIR spectrum of neat epoxy can be found. From 3400 to 1500 cm^{-1} , the peaks are achieved by hydroxyl, amino groups, asymmetric/symmetric C-H ($-\text{CH}_2$) stretching vibrations and amide $\text{C}=\text{O}$ stretching. Then, they are expected to be seen in spectra of all samples. But, theyir intensifies can be differ from sample to sample. Fewer than 1500 cm^{-1} wavenumber, occurred peaks are said to be sample specific. So, peaks at 1242, 1034, 826 and 700 cm^{-1} can be seen in Figure 5-7 as the specific absorbance bands of neat epoxy. Also, methyl groups ($-\text{CH}_3$) of epoxy are characteristics of bending vibration at 1385 cm^{-1} . The expectation from addition of filler material is that the chemical structure of neat epoxy should not be affected adversely.

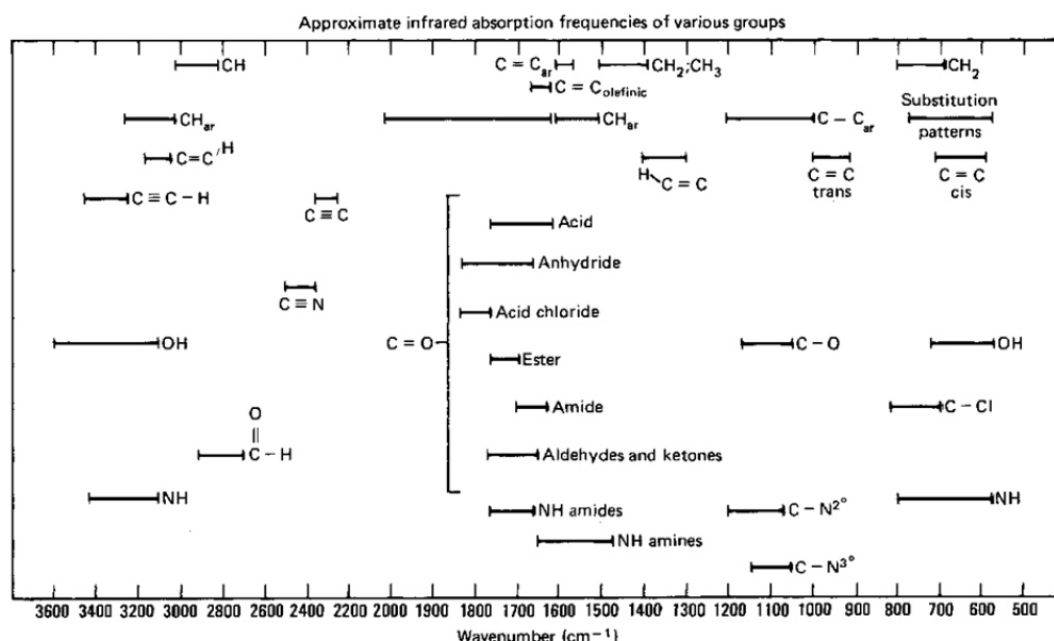


Figure 5-6 Reference FTIR Spectrum (http://what-when-how.com/wp-content/uploads/2011/06/tmp17058_thumb1.png)

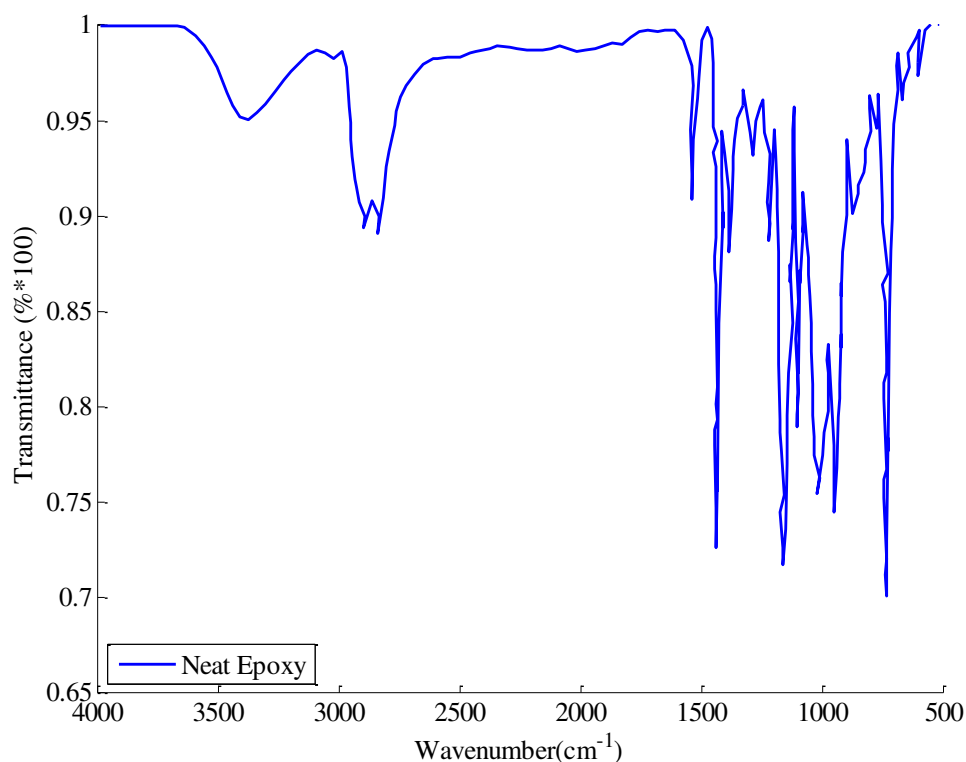


Figure 5-7 FTIR Spectrum of Neat Epoxy

In Figure 5-8, FTIR Spectra of hBN added composite structures can be seen. From 4000 to 1500 cm^{-1} , peaks show similarity with the neat epoxy. But, intensities are lowered by addition of hBN. At 1380 cm^{-1} , there can be seen a peak for hBN particles. This peak is the characteristics of B-N in-plane stretching vibration. Also, peak at 805 cm^{-1} represents the out of plane bending vibration of B-N. In addition, these peaks are said to be fingerprints of hBN particles.

In Figure 5-9, Epoxy composites with Al_2O_3 particles are examined by FTIR Spectroscopy. Like composites with hBN, functional groups' characteristic peaks are seen in the range of 4000-1500 cm^{-1} . Transmittance intensities show similarity with hBN and neat epoxy, as expected. At 731 and 610 cm^{-1} , the characteristic peaks of Al_2O_3 particles occur. In neat epoxy, there is also a small peak at 731 cm^{-1} . So, for the Al_2O_3 particles, characteristic is overlapped with neat epoxy.

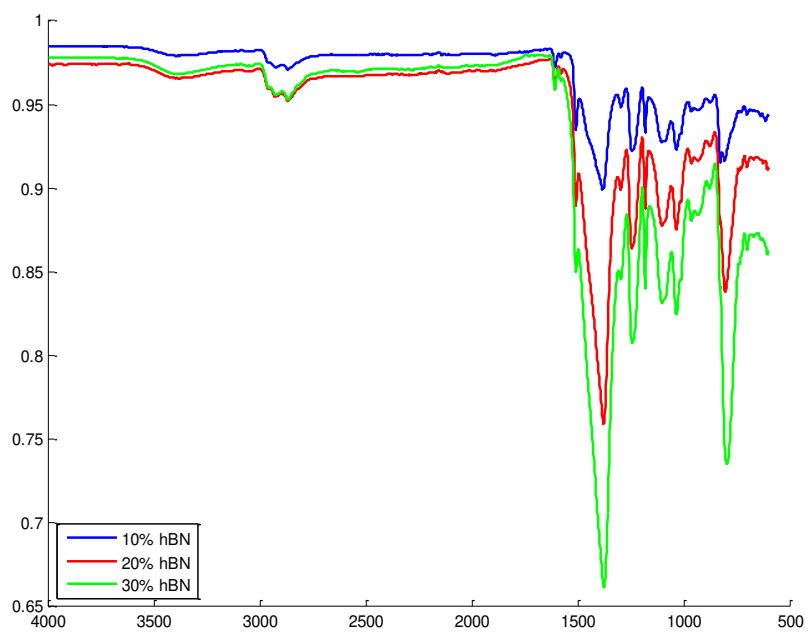


Figure 5-8 FTIR Spectra of Epoxy with hBN particles

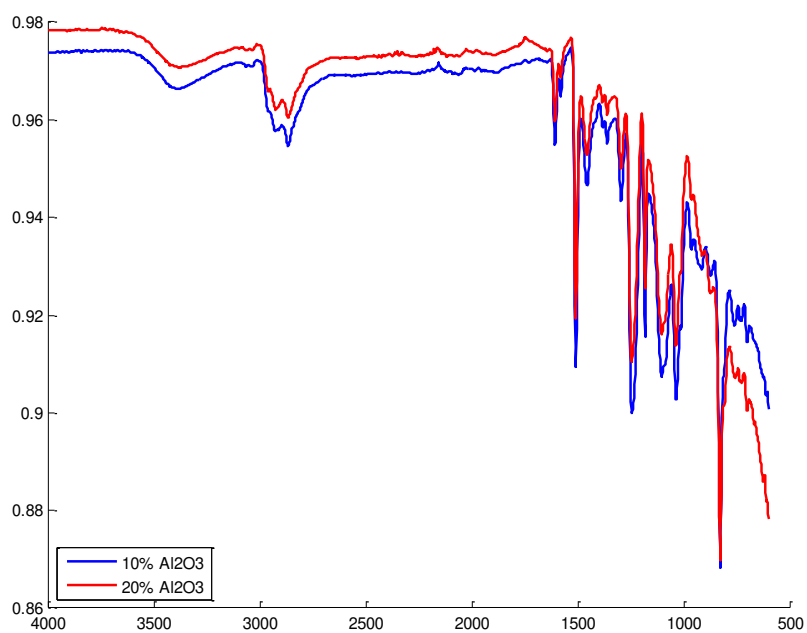


Figure 5-9 FTIR Spectra of Epoxy with Al₂O₃

In Figure 5-10, FTIR Spectra of synergetic mixtures of hBN and Al₂O₃ particles are shown. The peaks are common with other particles and neat epoxy for the range of 4000-1500 cm⁻¹. Since mixtures consist of hBN and Al₂O₃ particles, characteristic peaks of hBN and Al₂O₃ particles can be seen in these spectra. From 22.5-7.5 % hBN-Al₂O₃ to 24-6 % hBN-Al₂O₃, intensities are changed in favor of hBN particles' characteristic peaks by increasing hBN content.

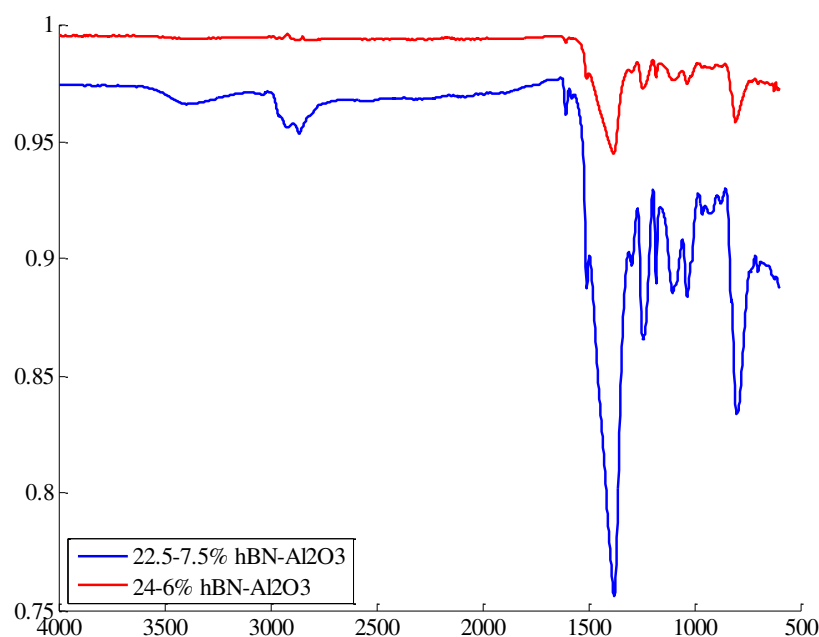


Figure 5-10 FTIR Spectra of Synergetic Mixtures of hBN and Al₂O₃

Epoxy composite with TiO₂ and Au-doped TiO₂ particles were also examined by FTIR Spectroscopy, as illustrated in Figure 5-11. The broad band from 500 to 900 cm⁻¹ is related to Ti-O-Ti and Ti-O-C stretching vibration. The characteristic peak of neat epoxy is matched with TiO₂ and Au-doped TiO₂ at 700 cm⁻¹ which is responsible for neat epoxy's OH groups. Therefore, in general, the coincidence of peaks between TiO₂ particles and neat epoxy can be seen clearly. In addition, Au particles only modify the intensity of peaks. Since all particles are nonfunctional and peaks show similarity with neat epoxy, it can be said that there is no modification in epoxy resin's chemical structure.

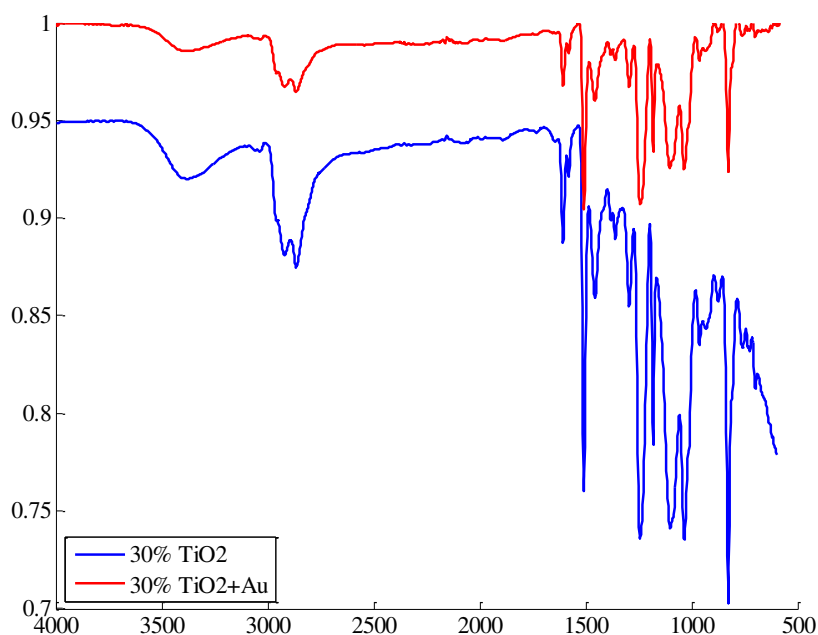


Figure 5-11 FTIR Spectra of TiO₂ and Au-doped TiO₂ Particles

With SEM screenings, morphological examination was conducted. The samples are frozen into liquid nitrogen. Then, they are broken into two pieces by diamond cutter. In addition, the cutting plane is needed to be flat and perpendicular to SEM plane. Since this operation is held manually, there can be misalignment and poor surface quality. Therefore, defects in screening and difficulty in identifying particles can occur inevitably. In Figure 5-12, SEM screening of sample with 20% hBN is shown. As seen, red arrows point the hBN particles. In addition, gaps in the samples can be indicated by red circles in figure. In Figure 5-13, sample with 20% Al₂O₃ particles topology is illustrated. Red circle in figure shows the Al₂O₃ particles and there is a huge agglomeration. Also, red arrows indicate the gaps on the cutting plane. Therefore, especially this agglomeration can worsen the performance of sample. Moreover, in Figure 5-14, SEM screening of epoxy with 24-6% hBN-Al₂O₃ particles is shown. Green arrows indicate the hBN particles and red arrows point the Al₂O₃ particles. In addition, red circles are where gaps occurred. Therefore, a local

agglomeration of Al_2O_3 particles is observed. On the other hand, hBN particles are distributed more evenly than hBN particles.

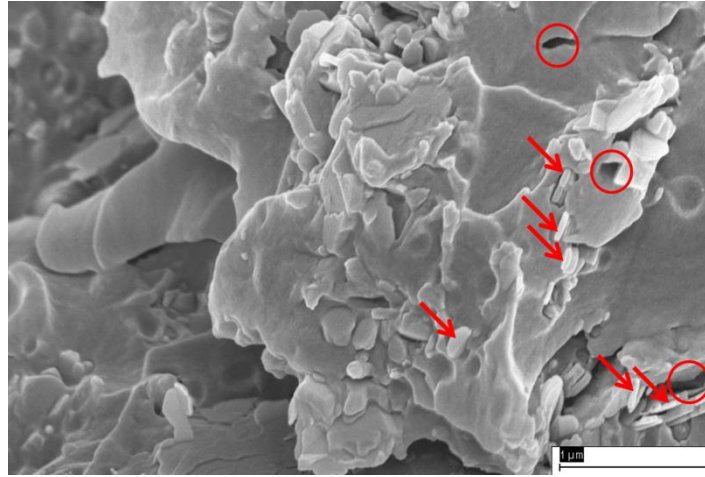


Figure 5-12 SEM Screening of 20% hBN

Finally, it can be said that a uniform distribution is hard to achieve in the composite adhesive. Some local agglomeration and gaps are admitted to be inevitable. This scanning process is aimed to see these agglomeration fields and gaps. Also, they should be kept at minimum rate as possible. As a result of these images, mixing process could be improved to distribute particles evenly.

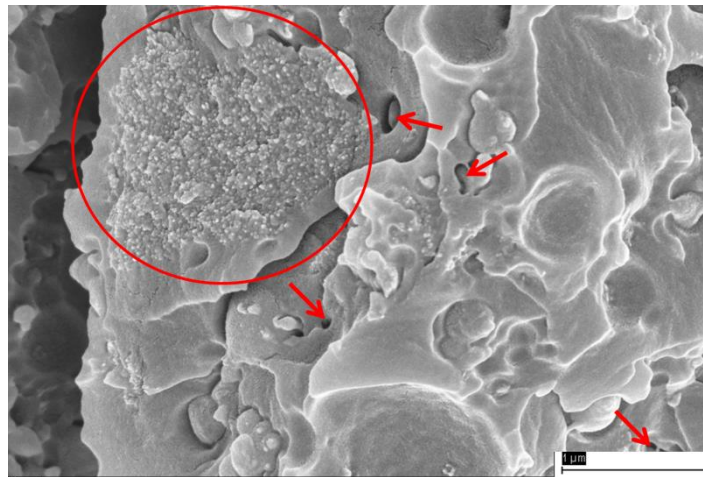


Figure 5-13 SEM Images of 20% Al_2O_3

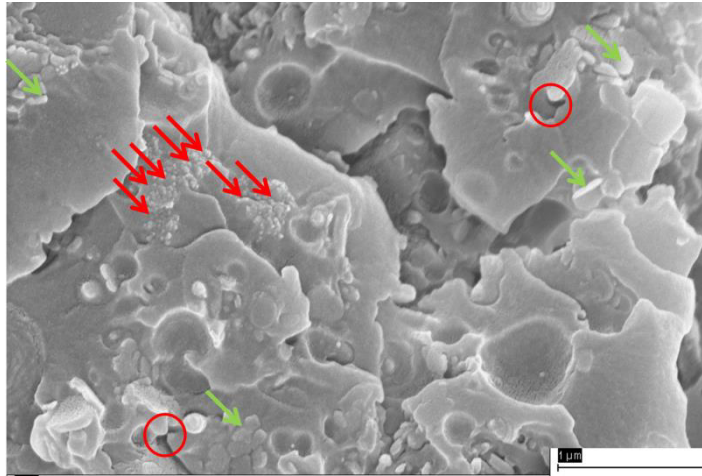


Figure 5-14 SEM Screening of Synergetic Mixture

Lastly, the single lap shear tests were conducted to determine adhesion strength. Test setup can be seen in Figure 5-15. These tests give information about mechanical properties of composite adhesive like DMA tests. Neat epoxy had the most ductile behavior. Since the filler materials are stiffer than epoxy, the samples with particles show less ductile behavior than neat epoxy. Moreover, the improvement in maximum shear stress is expected by addition of filler materials due to their relatively high stiffness values. In Table 5-3 given below, the maximum stress values for each sample is presented. The hBN and Al_2O_3 particles had favorable effects on maximum shear stress. On the contrary, the higher hBN and Al_2O_3 content decreased it. Moreover, TiO_2 particles affected the maximum shear stress adversely.

Shearing of adhesive joint includes two stages. First stage is the linear where behavior is elastic and second one is the plastic stage where behavior is inelastic. In Figure 5-16, an example of stress-strain curve is plotted. In the plot, point LL (linear limit) is the where elastic stage ends, KN (knee point) is the knee point where plastic stage becomes dominant and UL point is the ultimate stress point where breakage occurs.

Table 5-3 Maximum Shear Stress at Breakage of Samples

Sample	Maximum Stress (MPa)
Neat Epoxy	18.97
+10% hBN	19.74
+20% hBN	19.31
+30% hBN	16.42
+10% Al ₂ O ₃	20.86
+20% Al ₂ O ₃	16.33
+22.5-7.5% hBN-Al ₂ O ₃	17.45
+24-6% hBN-Al ₂ O ₃	18.35
+30% TiO ₂	14.71
+30% Au-doped TiO ₂	18.36



Figure 5-15 Single Lap Shear Test Setup

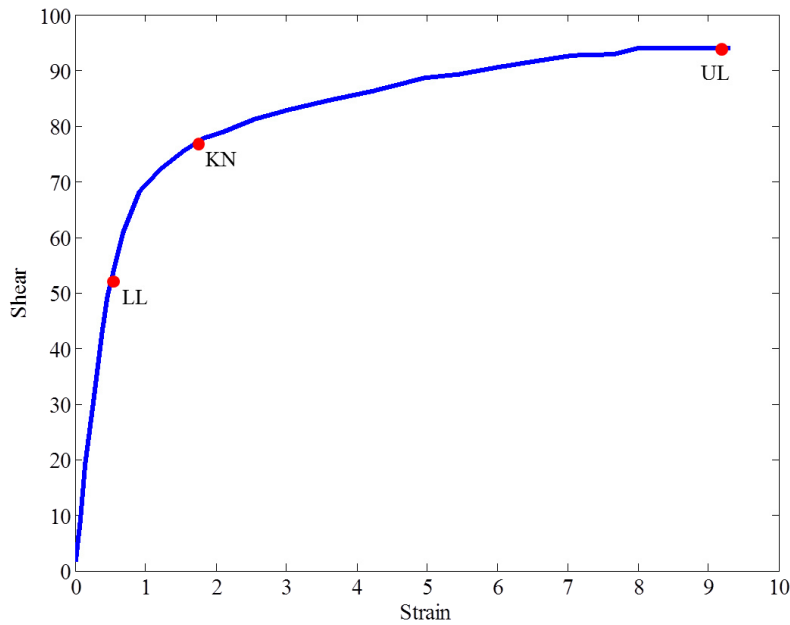


Figure 5-16 Example of Shear-Strain Curve

Neat epoxy's fracture surface is examined in Figure 5-17. There are three parts of adhesive joint, two adherends and an adhesive film. For successful testing, adhesive film is needed to be bonded with adherends. Also, fracture should occur in the adhesive film. For the neat epoxy sample, areas marked with red curves are places where bond between adhesive film and adherend is broken. Therefore, there can be a defect in sample preparation process. Moreover, dirt or dust on the adherends surfaces can affect the bonding between adherends and adhesive film adversely. In Figure 5-18, neat epoxy's stress-extension curve can be seen. All curves are divided into three in accordance with example stress-strain in Figure 5-16. In addition, LL and UL points of each curve are compared for performance enhancement. For the neat epoxy, the elastic limit is measured as 10 MPa from that curve and the ultimate stress point is 19 MPa.



Figure 5-17 Fracture Surface of Neat Epoxy

In Figure 5-18, shear stress over extension is plotted for neat epoxy and epoxy with Al_2O_3 particles. For 10wt% Al_2O_3 , the LL point is found as 13 MPa and UL point is 21 MPa. These values are 15 MPa and 16 MPa for 20wt% Al_2O_3 , respectively. Since addition of Al_2O_3 particles makes the composite adhesive stiffer, the UL point is expected to increase. The adherends are glued together with epoxy part of composite structure. Therefore, when there are particles in the interface area, lack of adhesion may occur. For this examination, the fracture surfaces should be investigated, which can be seen in Figure 5-19. Areas in red curves are where bonds between adherends and adhesive film are broken. For sample with 20wt% Al_2O_3 particles, this area is greater than the other sample. Therefore, underperformance of sample with 20wt% Al_2O_3 particles at ultimate stress point can be explained. Moreover, due to adhesion problem, the softening part of 20wt% Al_2O_3 content is limited and breakage occurred.

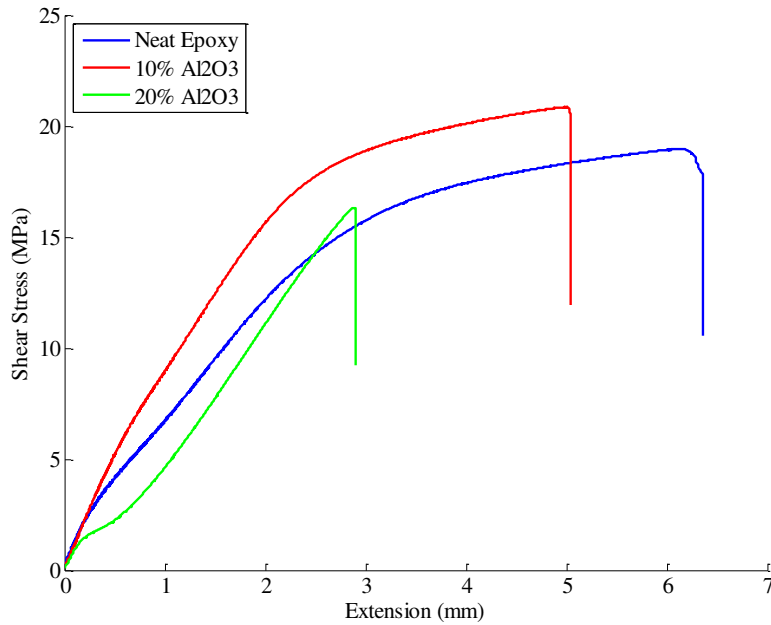


Figure 5-18 Al₂O₃ Particles' Effect on Shear Stress

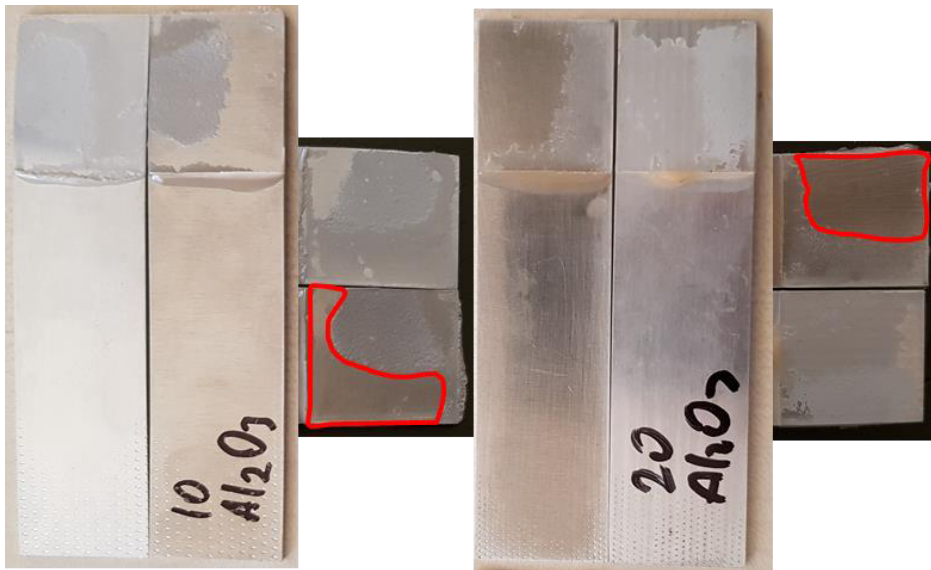


Figure 5-19 Fracture Surfaces of Al₂O₃ Samples

Effects of hBN particles on shear stress can be inferred from Figure 5-20. The linear limit points are 12 MPa for 10wt% hBN, 13 MPa for 20wt% hBN and 12 MPa for 30wt% hBN. In addition, the ultimate stress points are 20 MPa, 19 MPa and 16 MPa, respectively. The composite adhesive is cured as thin film between adherends.

Moreover, as hBN content increases, the possibility of placing hBN particles at interface also increases. Therefore, decrease in UL point can be explained by excessive particles in adhesive film. In addition, cross-linking is thought to occur between epoxy resin and particles. When amount of particles increases too much, agglomeration can occur. So, particles begin to contact with each other, and cross-linking is inhibited. Therefore, it is suspected as possible reason for decrease in elastic limit.

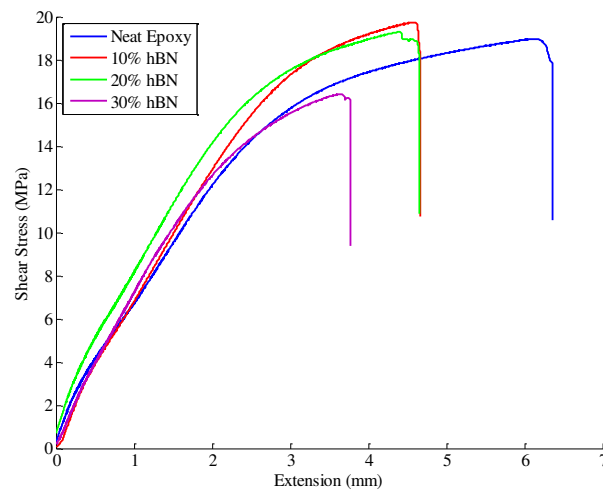


Figure 5-20 hBN Particles' Effect on Shear Stress

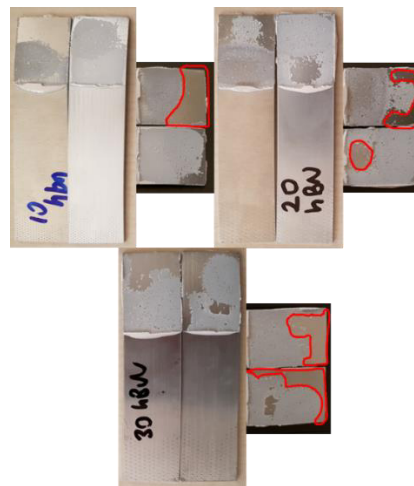


Figure 5-21 Fracture Surfaces of hBN Particles

In Figure 5-21, fracture surfaces of samples with hBN particles are shown. Enclosed areas with red curves are where de-bonding between adherends and adhesive film. As hBN content in composite adhesive increases, undesirable de-bonding areas increased. Since composite adhesive is cured as thin film, more hBN can cause the lack of bonding between adherends.

For the synergetic mixtures, shear stress-extension curves are shown in Figure 5-22. 12 MPa is the value of linear limit for epoxy with 22.5-7.5% hBN-Al₂O₃ particles. In addition, ultimate stress point is measured as 17.5 MPa. These values are 14 MPa and 18.3 MPa respectively for epoxy with 24-6% hBN- Al₂O₃ particles. From results, improvement in mechanical behavior is seen as hBN content increases. Since hBN has plate-like geometry which has extra area for interaction, the more cross-links occur between epoxy resin and particles.

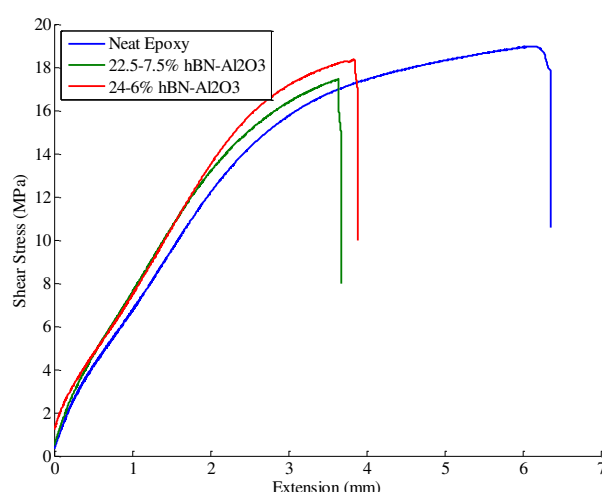


Figure 5-22 The Synergetic Mixture's Effect on Shear Stress

Stress behavior of samples can also be investigated by fracture surfaces which are shown in Figure 5-23. The de-bonding between adhesive film and adherends is much more in sample with 22.5-7.5% hBN-Al₂O₃ particles than other synergetic mixture. Since Al₂O₃ particles have higher stiffness than epoxy resin and hBN particles, the improvement is expected as Al₂O₃ content increases. From fracture surfaces, de-

bonding between adhesive film and adherends can explain the performance of sample with 22.5-7.5% hBN-Al₂O₃ particles.

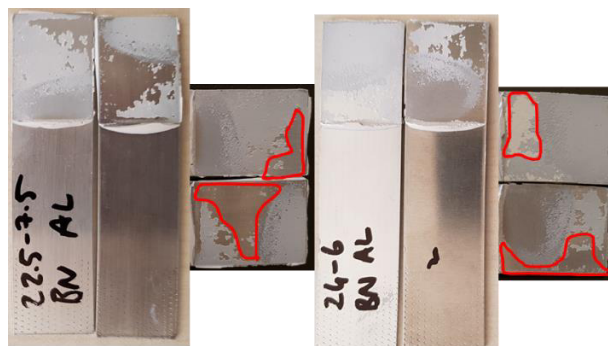


Figure 5-23 Fracture Surfaces of Synergetic Mixtures

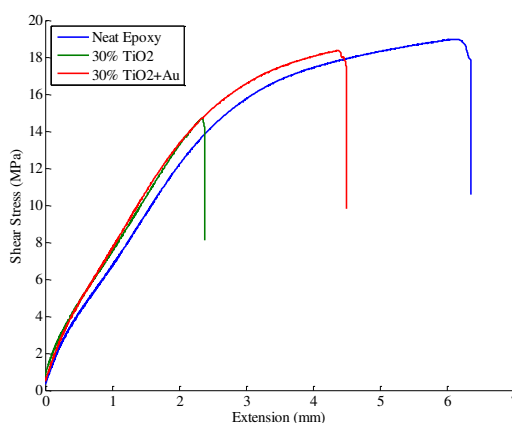


Figure 5-24 TiO₂ Particles' Effect on Shear Stress

In Figure 5-24, shear stress-extension curves of samples with TiO₂ and Au-doped TiO₂ particles are plotted. The linear limit is measured as 13 MPa for 30% TiO₂ particles and ultimate stress point is 14.7 MPa. These values are measured as 12.3 MPa and 18.3 MPa. The Au is doped to TiO₂ particles due to its greater thermal properties. Therefore, greater performance in mechanical behavior is not expected. From the results, elastic behavior is observed same for both samples, and it can be said that Au particles do not affect mechanical behavior adversely. In Figure 5-25, de-bonding area between adhesive film and adherend is almost as adhesive joint area for sample with TiO₂. So, the lower UL point for sample with TiO₂ particles can be

explained by excessive undesirable de-bonding area. The dust or dirt on adherend surface can be an excuse for this underperformance. Moreover, possible agglomeration of TiO_2 particles in adhesive film can make this happen.

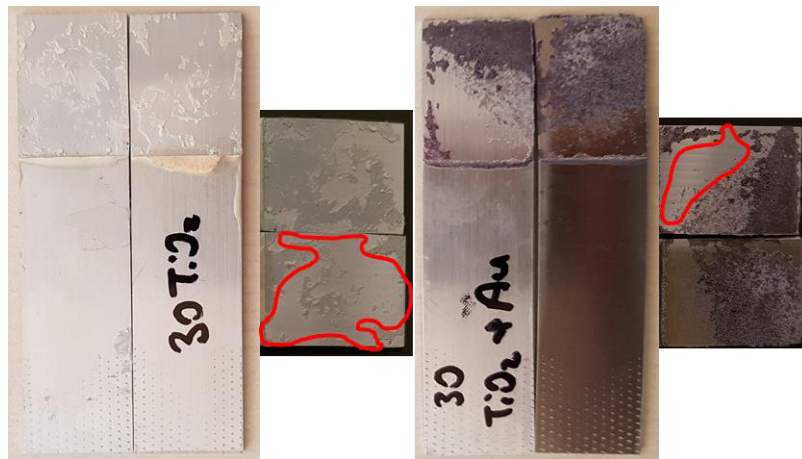


Figure 5-25 Fracture Surfaces of TiO_2 Particles

CHAPTER 6

CONCLUSIONS

In this study, commercially available epoxy adhesive, Loctite 9412, was used as epoxy matrix with the purpose of improving intrinsic properties by using filler materials as reinforcers. Then, nano-hBN, nano-Al₂O₃, nano-TiO₂ and nano-Au doped TiO₂ particles were used as filler materials. These particles were selected due to their individually great thermal and mechanical properties compared with epoxy adhesive. Thus, samples for each particle at different weight ratios were prepared. For the Al₂O₃ particles, 30 wt% ratio could not be prepared due to flocculation occurred while sample preparation. Also, hBN and Al₂O₃ particles were mixed to see any synergetic effect on the enhancement of epoxy adhesive. All samples were tested in order to determine thermal behavior by DMA, DSC and TC. Moreover, their morphologies were examined by SEM and FTIR Spectra. Also, their adhesion strengths were measured by Single Lap Shear Test. The preliminary work and test results were presented and published in [38,39].

The overall performance evaluation of composite adhesive is divided into thermal and mechanical behaviors, mainly. In order to determine the most favorable composition, thermal and mechanical properties should be balanced. Results show that adding particles have favorable influence on the thermal conductivity of composite adhesive structure. Since hBN particles have nearly 300 W/m.K of thermal conductivity, hBN particles have the most gain in thermal properties. Moreover, addition of 10, 20 and 30 wt% of hBN increases the thermal conductivity of neat epoxy from 0.18 W/m.K to 0.257, 0.319 and 0.386 W/m.K, respectively. For the Al₂O₃ added composite structures, thermal conductivity values are changed from 0.18 to 0.217 and 0.219 W/m.K for 10 and 20 wt% ratio of Al₂O₃ particles respectively. As expected, the synergetic mixture of hBN and Al₂O₃ particles also enhance the thermal conductivity value. The Al₂O₃ content in the mixture determines

conductivity of the samples. With 7.5 wt% Al_2O_3 sample has the thermal conductivity of 0.352 W/m.K while the one with 6 wt% has 0.343 W/m.K. Actually, values can be said as close to each other. hBN particles transmit heat in plane and Al_2O_3 particles transmit it omnidirectional. When these two particles interact, Al_2O_3 particles make heat transfer between hBN platelets easily possible. Therefore, the thermal pathways are well-constructed when interaction increases. It is thought that the difference between two samples can occur due to this phenomenon. Moreover, TiO_2 particles are known as additive material which enhances the thermal properties of composite adhesive structure. Addition of 30 wt% TiO_2 increases the thermal conductivity from 0.18 to 0.283 W/m.K. TiO_2 particles' thermal conductivity value is about 11.7 W/m.K, so this improvement is expected. On the other hand, Au doped TiO_2 particles worsen the composite adhesive structure's thermal conductivity which is 0.174 W/m.K. Au particles interacts with TiO_2 particles but there is bonding problem between epoxy matrix and Au particles. Because of that, there can be tiny gaps in composite adhesive structure. These particles precipitate because of their relatively high density which has poor influence on thermal pathways. Construction of thermal pathways is the key for the enhanced thermal properties. hBN platelets' thermal conductivity is over 1600 times great than neat epoxy, but their enhancement is limited to 200 times of neat epoxy. hBN particles' in plane heat transfer describes the heat transfer ratio. Therefore, adding Al_2O_3 to hBN should make possible construction of thermal pathways. If the optimal ratio between hBN and Al_2O_3 is found, the better thermal performance might be achieved.

DMA results give information about mechanical properties over temperature. The composite adhesive structures with hBN particles have poor mechanical properties than thermal ones. In service temperatures which is -35 to 55 °C, storage moduli of composite adhesive included 10 and 20 wt% hBN are lower than neat epoxy. For example, at 40 C°, neat epoxy's storage modulus is 0.87 GPa while 10 and 20 wt% samples have 0.74 and 0.70 GPa, respectively. Only 30 wt% of hBN has slightly improved behavior than neat epoxy. Al_2O_3 particles have better mechanical

properties. Their improvement can be seen in storage modulus results of composite adhesive structure. 20 wt% Al_2O_3 particles added composite adhesives have greater storage modulus value in whole service temperature range. For instance, at 40 °C, composite adhesive has storage modulus of 0.92 GPa. On the other hand, before 45 °C, 10 wt% Al_2O_3 particles' storage modulus is lower than neat epoxy, which is value of 0.8 GPa. The synergetic mixture of 24 wt% hBN and 6 %wt Al_2O_3 has better storage modulus before 45 °C and same behavior after that. At 40 °C, its storage modulus is value of 0.91 GPa. In addition, the other synergetic mixture's storage modulus is matched with neat epoxy's one in service temperature range. All TiO_2 included composite adhesives have poor storage modulus than neat epoxy. For example, again at 40 °C, TiO_2 added composite adhesive has storage modulus of 0.69 GPa and Au doped TiO_2 added one has it of 0.67 GPa. In summary, Al_2O_3 particle added composite structure has the best storage modulus behavior. Al_2O_3 particles have great mechanical properties over temperature, so with the harmony between particles and epoxy matrix, the composite adhesive structure's mechanical properties can be improved.

One of the determining specifications is the T_g value and it is determined from the DSC results. It is highly effective on the service temperature. Moreover, it decides whether an epoxy can be used or not. Neat epoxy's T_g value is measured as 44.54 °C. hBN particles added composite structures have the values of 45.82, 47.08 and 49.73 °C for 10, 20 and 30 wt% ratios respectively. Moreover, Al_2O_3 included adhesives' T_g values are 47.73 and 47.98 °C for 10 and 20 wt% ratios accordingly. The synergetic mixture of 22.5 wt% hBN and 7.5 wt% Al_2O_3 has the T_g value of 49.00 °C while the other synergetic mixture has the value of 47.04 °C. Finally, TiO_2 derivatives have T_g values of 51.55 and 55.92 °C. The latter is the result for Au doped TiO_2 . TiO_2 particles have the most brilliant results among all samples. When service temperature range is considered, Au doped TiO_2 particle added composite adhesives take the lead.

SEM images are valuable tools to figure out inner structure of the samples. It can be easily seen whether agglomeration occurred or not. Also, they give information about gap presence in epoxy matrix and at the edges of particles. Gaps are obstacles to heat transfer through the composite adhesive. Same samples used in DMA tests are used for SEM scanning. They are waited in liquid nitrogen for a while. Then, they are broken into two pieces. But cutting process is held by an operator. Also, it is a way difficult to have flat and perpendicular cutting plane by hand. In this study, SEM images indicate that agglomeration problems cannot be avoided completely. Also, some gaps are shown in SEM screenings. In addition, there is not observed wetting problem at the edges of particles in broken faces. Moreover, FTIR spectra can be counted as a tool for inner structure inspection. FTIR spectrum inspects the atomic bonds in the composite adhesive. It shows presence of expected bonds between particles and epoxy matrix in association with SEM images. Also, change in chemical structure of epoxy matrix can be investigated by comparing spectra of neat epoxy and other samples. In this study, FTIR spectrum is compared with the reference spectrum and FTIR spectra of samples with filler particles showed similarity with neat epoxy. Therefore, addition of filler material did not deform the chemical structure of neat epoxy.

For the characterization, the appropriate mechanical tests should be conducted. The single lap shear test is the one of most common characterization tests for adhesives. While DMA results give information about mechanical properties over temperature, single lap shear test shows purely mechanical properties. After shear tests, fracture surfaces of samples are also investigated. Breakage of bond is needed in adhesive film to investigate adhesive's shear performance. For the samples used in this work, breakage between adhesive film and adherends are observed. Therefore, samples can have lack of shear performance and the results may be misleading. In addition, possible reasons for having improper de-bonding can be dirt or dust on adherend surface. Surface roughness can also be a suspect. Another possible reason for poor bonding is the thickness of adhesive film. When the thickness is decreased, particles

can be placed on the adherend's surface. Therefore, in these locations, bonding may not be occurred. Moreover, from results, elastic limits are enhanced by addition of filler materials. Improvement in elastic limit is mostly achieved by Al_2O_3 particles as expected due to their high mechanical properties. Unlike the assumption, with increasing Al_2O_3 particles, elastic limit is decreased. Since fracture surface of sample with 20wt% Al_2O_3 particles had more area of de-bonding between adherends and adhesive film, this weakening could be explained. Also, the highest ultimate stress point was obtained by Al_2O_3 particles. For the other particles, performance of hBN particles was decreased with increasing hBN particles. When the fracture surfaces were investigated, unwanted de-bonding was also increased with increasing amount of particles. For the case study, the displacement in joint is undesirable. Hence, the samples with higher elastic limit are chosen. In this work, epoxy with 10wt% Al_2O_3 particles has the best configuration for mechanical performance.

After all, in this study, a delicate sample preparation method is expressed and examined by the SEM and FTIR analysis. Also, developing a sophisticated adhesive for aerospace applications is aimed. In order to achieve this goal, an epoxy resin is enriched with different types of additive materials. The additive materials are selected from the literature to confirm and improve findings. All prepared samples are tested by DMA, DSC and Thermal Inductivity Measurement, so their thermal behavior can be compared. Then, they are tested by single lap shear test to see their mechanical behavior. From among all samples, hBN particles are mostly contributed to thermal conductivity. In addition, Al_2O_3 particles have great influence on adhesion strength. Results of T_g values imply that TiO_2 derivatives show the necessary enhancement to work in service temperature range. In this case study, it is important that adhesive joint should preserve its structural integrity at extremity of service temperature. Also, thermal conductivity of adhesive joint should be improved to contribute structural integrity during heat cycles. Since there is no significant static loads on adhesive joint, 30 wt% TiO_2 shows better performance even if its mechanical properties is not great as the other samples. With this study, it

is shown that an advanced adhesive can be developed by reinforcing the epoxy adhesive by filler materials. For further applications, the composite adhesive with Au doped TiO₂ particles can be produced by eliminating the precipitation problem. Then, expected thermal performance should be achieved.

REFERENCES

- [1] Bishopp, J. (2005). Chapter 5 Aerospace: A pioneer in structural adhesive bonding. In *Handbook of Adhesives and Sealants* (pp. 215–347). Elsevier. [https://doi.org/10.1016/s1874-5695\(02\)80006-9](https://doi.org/10.1016/s1874-5695(02)80006-9)
- [2] de Bruyne, N. A. (1987). *Pioneering Times*. Techne Inc., Princetown, NJ.
- [3] Pate, K. D. (2002), Applications of adhesives in aerospace. In: M. Chaudhury, & A. V. Pocius (Eds), *Adhesion Science and Engineering (Chemistry and Applications, Vol. 2*, pp. 1128-1192), Elsevier, Amsterdam
- [4] Katsiropoulos, C. V., Chamos, A. N., Tserpes, K. I., & Pantelakis, S. G. (2012). Fracture toughness and shear behavior of composite bonded joints based on a novel aerospace adhesive. *Composites Part B: Engineering*, 43(2), 240–248. doi:10.1016/j.compositesb.2011.07.010
- [5] James, L & Dale, S. (2011). *Adhesives Technology for Electronic Applications*. Adhesives Technology for Electronic Applications. 10.1016/C2009-0-64364-6.
- [6] R. Qian, J. Yu, C. Wu, X. Zhai, P. Jiang, Alumina-coated graphene sheet hybrids for electrically insulating polymer composites with high thermal conductivity, *RSC Advances*. 3 (2013) 17373.
- [7] M. Shioya, Y. Kuroyanagi, M. Ryu, J. Morikawa, Analysis of the adhesive properties of carbon nanotube- and graphene oxide nanoribbon-dispersed aliphatic epoxy resins based on the Maxwell model, *International Journal of Adhesives and Adhesion*. 84 (2018) 27–36.
- [8] X. Huang, X. Qi, F. Boey, H. Zhang, Graphene-based composites, *Chemical Society Review*. 41 (2012) 666–686.
- [9] M. Hussain, A. Nakahira, K. Niihara, Mechanical property improvement of carbon fiber reinforced epoxy composites by Al₂O₃ filler dispersion, *Material Letters* 26 (1996) 185–191.
- [10] Q. Mu, S. Feng, G. Diao, Thermal conductivity of silicone rubber filled with ZnO, *Polymer Composites* 28 (2007) 125–130.
- [11] Wattanakul, K., Manuspiya, H., & Yanumet, N. (2011). Thermal conductivity and mechanical properties of BN-filled epoxy composite: effects of filler content, mixing conditions, and BN agglomerate size. *Journal of Composite Materials*, 45(19), 1967–1980. <https://doi.org/10.1177/0021998310393297>
- [12] Singh, S. K., Singh, S., Kumar, A., & Jain, A. (2017). Thermo-mechanical behavior of TiO₂ dispersed epoxy composites. *Engineering Fracture Mechanics*, 184, 241–248. <https://doi.org/10.1016/j.engfracmech.2017.09.005>

- [13] W. Jiao, Y. Liu, G. Qi, Studies on mechanical properties of epoxy composites filled with the grafted particles PGMA/Al₂O₃, *Composite Science Technology* 69 (2009) 391–395.
- [14] Bian, W., Yao, T., Chen, M., Zhang, C., Shao, T., & Yang, Y. (2018). The synergistic effects of the micro-BN and nano-Al₂O₃ in micro-nano composites on enhancing the thermal conductivity for insulating epoxy resin. *Composites Science and Technology*, 168, 420–428. <https://doi.org/10.1016/j.compscitech.2018.10.002>
- [15] K. Kim, M. Kim, Y. Hwang, J. Kim, Chemically modified boron nitride-epoxy terminated dimethylsiloxane composite for improving the thermal conductivity, *Ceramics International* 40 (2014) 2047–2056.
- [16] Zhou, W., Zuo, J., Zhang, X., & Zhou, A. (2013). Thermal, electrical, and mechanical properties of hexagonal boron nitride–reinforced epoxy composites. *Journal of Composite Materials*, 48(20), 2517–2526. <https://doi.org/10.1177/0021998313499953>
- [17] Peng, W. Y., Huang, X. Y., & Yu, J. H. Electrical and thermophysical properties of epoxy/aluminum nitride nanocomposites: Effects of nanoparticle surface modification. *Composites Part A* 2010; 41: 1201–1209.
- [18] Ekrem, M., Şahin, Ö. S., Karabulut, S. E., & Avcı, A. (2017). Thermal stability and adhesive strength of boron nitride nano platelets and carbon nano tube modified adhesives. *Journal of Composite Materials*, 52(11), 1557–1565. doi:10.1177/0021998317726147
- [19] Kim WS, Yun IH, Lee JJ, et al. Evaluation of mechanical interlock effect on adhesion strength of polymer-metal interfaces using micro-patterned surface topography. *International Journal of Adhesives and Adhesion* 2010; 30:408–417.
- [20] Brown, G. M., & Ellyin, F. Assessing the predictive capability of two-phase models for the mechanical behavior of alumina/epoxy nanocomposites. *Journal of Applied Polymer Science* 2005;98:869–879.
- [21] Brown, G. M., & Ellyin, F. Mechanical properties and multiscale characterization of nanofiber-alumina/epoxy nanocomposites. *J. Appl. Polym. Sci.* 2011;119:1459–1468.
- [22] Miyagawa, H., Mohanty, A., Drzal, L. T., & Misra, M. Effect of clay and alumina-nanowhisker reinforcements on the mechanical properties of nanocomposites from biobased epoxy: a comparative study. *Industrial and Engineering Chemistry Research* 2004;43:7001–7009.
- [23] Zhao, S., Schadler, L. S., Duncan, R., Hillborg, H., & Auletta, T. Mechanisms leading to improved mechanical performance in nanoscale alumina filled epoxy. *Composite Science Technology* 2008;68:2965–975.

- [24] Wetzel, B., Rosso, P., Hauptert, F., & Friedrich, K. Epoxy nanocomposites – fracture and toughening mechanisms. *Engineering Fracture Mechanics* 2006;73:2375–2398.
- [25] Johnsen, B. B. , Frømyr , T. R., Thorvaldsen, T., & Olsen, T. (2013) Preparation and characterisation of epoxy/alumina polymer nanocomposites, *Composite Interfaces*, 20:9, 721-740, DOI: 10.1080/15685543.2013.815603
- [26] Song, B., Chen, W., Montgomery, S. T., & Forrestal, M. J. (2009), Mechanical Response of an Alumina-filled Epoxy at Various Strain Rates. *Journal of Composite Materials*, 43(14), 1519-1536. <https://doi.org/10.1177/0021998308337741>
- [27] Jiang, W., Jin, F.-L., & Park, S.-J. (2012). Thermo-mechanical behaviors of epoxy resins reinforced with nano-Al₂O₃ particles. *Journal of Industrial and Engineering Chemistry*, 18(2), 594–596. <https://doi.org/10.1016/j.jiec.2011.11.140>
- [28] Hu, Y., Du, G., & Chen, N. (2016). A novel approach for Al₂O₃ /epoxy composites with high strength and thermal conductivity. *Composites Science and Technology*, 124, 36–43. <https://doi.org/10.1016/j.compscitech.2016.01.010>
- [29] J.-W. Bae, W. Kim, S.-H. Cho, S.-H. Lee, The properties of AlN-filled epoxy molding compounds by the effects of filler size distribution, *Journal of Material Science* 35 (23) (2000) 5907e5913.
- [30] Zhai, L., Ling, G., Li, J., & Wang, Y. (2006). The effect of nanoparticles on the adhesion of epoxy adhesive. *Materials Letters*, 60(25-26), 3031–3033. doi:10.1016/j.matlet.2006.02.038
- [31] Stawarz, S., Witek, N., Kucharczyk, W., Bakar, M., & Stawarz, M. (2018) Thermo-protective properties of polymer composites with nano-titanium dioxide. *International Journal of Mechanics and Materials Design*. <https://doi.org/10.1007/s10999-018-9432-7>
- [32] Al-Ajaj, L. A., Abd, M. M., & Jaffer, H. I. (2013). Mechanical Properties of Micro and Nano TiO₂/Epoxy Composites, *International Journal of Manufacturing Material and Mechanical Engineering*, 1, ISSN 2320-4060
- [33] Merad, L., Benyoucef, B., Abadie, M. J. M., & Charles, J. P. (2011). Characterization and Mechanical Properties of Epoxy Resin Reinforced with TiO₂ Nanoparticles. *Experimental Techniques*, 38(1), 59-66. <https://doi.org/10.1111/j.1747-1567.2011.00797.x>
- [34] Sahu, M., & Satapathy, A. (2014). A Study on Microsized Titanium Oxide-Filled Epoxy with Enhanced Heat Conductivity for Microelectronic Applications. *Particulate Science and Technology*, 33(1), 109–112. <https://doi.org/10.1080/02726351.2014.941081>

- [35] Kumar, K., Ghosh, P. K., & Kumar, A. (2016). Improving mechanical and thermal properties of TiO₂-epoxy nanocomposite. *Composites Part B: Engineering*, 97, 353–360. <https://doi.org/10.1016/j.compositesb.2016.04.080>
- [36] Tutunchi, A., Kamali, R., & Kianvash, A. (2014). Steel-Epoxy Composite Joints Bonded with Nano-TiO₂ Reinforced Structural Acrylic Adhesive. *The Journal of Adhesion*, 91(9), 663–676. doi:10.1080/00218464.2014.961187
- [37] Veziroglu, S., Ghorri, M. Z., Kamp, M., Kienle, L., Rubahn, H.-G., Strunskus, T., & Aktas, O. C. (2018). Photocatalytic Growth of Hierarchical Au Needle Clusters on Highly Active TiO₂ Thin Film. *Advanced Materials Interfaces*, 5(15), 1800465. doi:10.1002/admi.201800465
- [38] Yalçınkaya, T. (2019). Synthesis and Characterization of Epoxy/Boron Nitride Composite for Aerospace Applications. *Journal of Aeronautics and Space Technologies*, 12(1), 87-94.
- [39] Yetgin, H., Veziroglu, S., Aktas, O. C., & Yalcinkaya, T. (2019) High Thermal Conductive Epoxy Composites with a Binary-Particles System of h-BN and Al₂O₃ nanoparticles. *International Journal of Adhesion and Adhesives*, 98, doi:10.1016/j.ijadhadh.2019.102540